MUSCLE MECHANICS AND ULTRASTRUCTURE I

M-AM-A1

ATP HYDROLYSIS RATE AND TENSION DEVELOPMENT IN RAT CARDIAC TRABECULAE: INFLUENCE OF TEMPERATURE. ((**P.P. de Tombe** and G.J.M. Stienen)) Dept. of Physiology and Biophysics, University of Illinois at Chicago, Chicago IL 60612, and Laboratory for Physiology, Free University Amsterdam, The Netherlands.

The influence of temperature on the rate of cross-bridge cycling and tension development was studied in cardiac trabeculae isolated from rat hearts. The trabeculae (n=8) were skinned overnight (1% Triton-X100 in relaxing solution). Resting sarcomere length was measured by laser diffraction, and maintained at 2.3 μm. ATPase activity was measured on-line by an enzyme coupled NADH absorbance assay and expressed per fiber volume. Force development was studied over a wide range by changing the free calcium concentration in the activating solution; data were collected at 15, 20, and 25 C. Maximum tension (force devided by cross-sectional area) varied only slightly with temperature: 32.6±1.0, 45.0±0.7, and 47.5±3.0 mN/mm^2 at 15,20, and 25 C, respectively (Q_{10}=1.3±.0.1). The average relationship between tension development and ATP hydrolysis rate at the three temperatures is shown in Figure A. The slope of this relationship, which represents the energetic cost of force maintenance (1/economy) was independent of the free [Ca^{2+}], and increased significantly with temperature: 5.4±0.8, 9.0±0.9, and 15.6±1.7 μM•s^{-1}•mN^{-1}•mm^2,respectively. Arrhenius plots of these data (Figure B) revealed an activation energy of 71.2±3.3 kJ•mol^{-1}, which is equivalent to a Q_{10} of 2.7±0.1 over this temperature range. We conclude that myocardial cross-bridge cycling is highly temperature dependent.

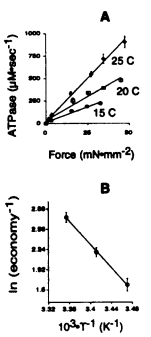

M-AM-A2

MOTIONS OF BIFUNCTIONAL RHODAMINE PROBES WITH DEFINED ORIENTATIONS ON THE REGULATORY LIGHT CHAIN (RLC) IN SKELETAL MUSCLE FIBERS ((**S.C. Hopkins**, [C]C. Sabido-David, *B.D. Brandmeier, [†]J. Kendrick-Jones, [C]R.E. Dale, *J.E.T. Corrie, *D.R. Trentham, [C]M. Irving and Y.E. Goldman)). Penna. Muscle Institute., Univ. of Penna., Philadelphia, USA; [C]Randall Institute, King's College London, UK; *NIMR, London NW7 1AA, UK; [†]MRC LMB, Cambridge, UK.

Motions of myosin heads related to force generation and protein elasticity were produced by quick length changes in rabbit psoas fibers containing RLC mutants labeled with bifunctional rhodamine (BR; Sabido-David et al., this meeting). Fluorescence polarization ratios (Q), measured at 50 μs time resolution, were interpreted in terms of two orientational order parameters and restricted rotational mobility on the fluorescence timescale (Dale et al., this meeting). With quick releases in active contraction, 100-BR-108 (parallel to the heavy chain helix near the RLC) and 104-BR-115 tilt toward the rigor orientation more perpendicular to the fiber axis. This motion is consistent with the power stroke ending near the rigor orientation. 108-BR-113 tilts much less, suggesting that this probe is roughly normal to the tilt plane of the RLC. During quick tension recovery after stretch, 100-BR-108 tilts in the same direction as during the step, but 104-BR-115 recovers towards the isometric orientation. All the length step responses were small ($\Delta Q < 0.05$) compared to those expected if most of the cross-bridges execute a conventional working stroke, suggesting that a small fraction tilts in response to the steps. With stretch in rigor all three probes tilt towards the active orientation. The distinct responses of 108-BR-113 in active contraction and rigor suggest that the orientation of the RLC relative to the tilt plane is markedly different in these two states. Supported by AR26846 and the MDA, USA; Wellcome Trust and MRC, UK.

M-AM-A3

TWO DISTINCT ORIENTATIONS OF SPIN-LABELED REGULATORY LIGHT CHAINS IN CONTRACTING SCALLOP MUSCLE FIBERS.
((Josh E. Baker, Ingrid Brust-Mascher, Sampath Ramachandran, David D. Thomas)) University of Minnesota, Minneapolis, MN 55455

We have used electron paramagnetic resonance (EPR) to study orientational changes in the light-chain binding domain of myosin during muscle contraction. The native regulatory light chain (RLC) was extracted from skinned scallop adductor muscle fibers, and the fibers were reconstituted to full calcium-sensitivity with gizzard RLC labeled with fluorodinitroaniline spin label (FDNASL) at Cys 108. EPR spectra were resolved into two components having distinct probe orientations of 44° and 76° relative to the fiber axis. Changing the physiological state of the muscle fiber resulted in a change in the distribution between these two components. In the absence of ATP (rigor), the 44° component is predominant. In the presence of ATP (relaxation), the distribution shifts toward the 76° component. In the presence of ATP and Ca^{2+} (contraction), the proportions of these two populations are intermediate between rigor and relaxation. Thus, force generation appears to involve a change in the distribution between these two states of LC domain orientation. **These results constitute the first direct evidence for two distinct myosin head angles in muscle fibers.** Since previous studies of spin labels bound to the catalytic domain (in vertebrate muscle) showed only one distinct orientation, these results suggest that the LC domain rotates relative to the catalytic domain.

M-AM-A4

Cross-bridge conformation during isometric contraction and in the presence of nucleotide analogs: a 2D-X-ray diffraction study on single muscle fibers.
((Th. Kraft, B. Brenner)) Medical School, 30625 Hannover, Germany.

To further understand the mechanism of force generation in skeletal muscle, we set out to study the structural changes that occur during active cross-bridge cycling. The questions was: During isometric contraction is there a significant population of rigor-like cross-bridges representing the force generating cross-bridge states (cf. Rayment et al., Science 261, 1993)?
In order to investigate this question (1) we recorded 2D-X-ray diffraction patterns under maximum activation (pCa 4.5) and studied the structural features of strongly bound states as they exist during isometric contraction. We used single fibers to avoid ATP depletion problems and mounted 30 single fibers together into the setup to obtain sufficient intensity to record equatorial, meridional and layer line reflections. The patterns were recorded during the isometric steady state period of a quick release protocol (Brenner, BJ.41, 1983) and no evidence for a detectible fraction of cross-bridges occupying a rigor-like conformation was found. (2) A titration of ATPgS in the presence of calcium was carried out to study the features of different mixtures of nucleotide-free (rigor-like) and weakly bound cross-bridges in 2D-X-ray diffraction patterns. None of these patterns, however, was comparable to the patterns under isometric contraction, thus making it unlikely that the isometric steady state represents a mixture of weak binding and strongly attached rigor-like heads. (3) 2D-X-ray diffraction patterns were recorded in the presence of nucleotide analogs representing strong binding cross-bridge states, such as $MgPP_i$ to characterize typical features of strong binding states other than rigor-like cross-bridges.

M-AM-A5

X-RAY DIFFRACTION STUDIES OF THE ACTIN-MYOSIN INTERACTION DURING HIGH VELOCITY SHORTENING OF SINGLE FROG MUSCLE FIBRES.

((M. Reconditi[1], G. Piazzesi[1], I.Dobbie[2], M. Irving[2], P. Bösecke[3], O. Diat[3], M. Linari[1], & V. **Lombardi**[1])) [1]Dip. Scienze Fisiologiche, Università di Firenze, 50134 Firenze, Italy; [2]The Randall Institute, King's College London, London WC2B 5RL, U.K.; [3]ESRF, BP 220, F-38043 Grenoble Cedex, France. (Spon. by N.A. Curtin)

Low angle x-ray diffraction patterns were recorded from intact single fibres of frog tibialis anterior muscle during active shortening near the maximum velocity (V_0), sarcomere length ~2.2μm, 4 °C, using a 10m camera at the ID2(SAXS) station at ESRF. The shortening ramp was imposed at the plateau of an isometric tetanus. At the start of ramp shortening the intensity of the 3rd order meridional reflection (M3), which is sensitive to the axial orientation of the myosin cross-bridges, decreased to ca. 15% of its isometric plateau value, with the same time course as the tension decrease. The spacing of the M3 reflection also decreased to 14.40nm, intermediate between the plateau value of 14.57nm and the resting value of 14.34nm, with a delay of ~10ms with respect to the tension decrease. This delay corresponds to about 20nm of filament sliding. At the isometric plateau the intensities of both the 1st order myosin layer line at 43nm and of the 2nd order meridional cluster at ca. 21.5nm were less than 10% of their resting values. These intensities did not change significantly during the first 10ms of shortening near V_0, but subsequently increased to 30-40% of their resting values with the same time course as the decrease in M3 spacing. All these changes were fully reversed during isometric tension redevelopment after the end of shortening. These results suggest that the cross-bridges that were attached at the isometric plateau tilt axially during the first 20nm of filament sliding, and that the appearance of diffraction features characteristic of resting muscle is delayed until these cross-bridges have completed their working stroke. Supported by EC, CNR (Italy), MRC (UK), ESRF and EMBL.

M-AM-A6

TITIN ELASTICITY: LASER TRAP MEASUREMENT OF FORCE-EXTENSION CURVES OF ISOLATED TITIN MOLECULES

((K. Wang, J. Wright, G. Gutierrez, A. Brady, M. Sheetz*)) Univ. of Texas, Austin, TX and *Duke Univ. Med. Center. Durham, NC.

The direct measurement of force-extension relationship of individual titin molecules is essential to the understanding of the molecular basis of titin and muscle elasticity. Minute molecular forces comparable to the yield point tension of titin (25-50 pN per rabbit psoas titin, Wang et al. PNAS *88*, 7101) can be measured with high sensitivity by laser trap techniques. Studies on isolated rabbit psoas titin (T2) with a single-beam optical trap have demonstrated this feasibility. In early attempts to use a pair of mAb's with known epitope loci to attach titin to latex beads, we found titin-tethered beads dissociated frequently. Therefore the more enduring biotin-avidin interaction is used subsequently. The tethers are formed by first adsorbing 1 μm streptavidin beads to a glass coverslip, blocked, followed by biotinylated titin and then 0.5 μm streptavidin-beads. We have succeeded in reversibly stretching titin by as much as 0.4 μm ,with the smaller bead trapped by the laser beam. The deflection of the trapped bead from the center of the trap is, within limits, a measure of the elastic force of the titin. The force-extension curves clearly indicate that they are exponential up to 20-30 pN for native titin in aqueous solution. Unexpectedly, unfolding of titin by 6-8 M urea had no apparent effect on the functional form of force-extension curves. Our data suggest that titin is a non-Hookeain spring that extends easily at low force and stiffens significantly at higher extension. The unfolding experiments suggest that an elastic component of titin is robust and barely affected by urea. PEVK segment may be such an elastic element (supported by NIHAR43514 and FFR).

M-AM-A7

ELASTIC PROPERTIES OF THE TITIN MOLECULE MEASURED USING AN OPTICAL TRAP.

((**Miklós S.Z. Kellermayer**, Steven B. Smith*, Henk L. Granzier, and Carlos Bustamante*†)) Department of VCAPP, Washington State University, Pullman, WA 99164-6520; *Institute of Molecular Biology, †Howard Hughes Medical Institute, University of Oregon, Eugene, OR 97403.

Titin (also known as connectin) is a giant filamentous protein that spans the distance between the Z- and M-lines of the vertebrate muscle sarcomere. Several indirect observations have implicated titin as playing a fundamental role in the generation of passive force of muscle, driven by titin's elastic properties. A direct measurement of the mechanical properties of titin, however, has not been documented. Ideally, one would want to measure these properties on a single isolated molecule under conditions where the effect of components associated with titin are absent. Here we present force-length relations for single titin molecules mounted between two microscopic beads (2-3 μm) coated with specific anti-titin antibodies (T12 or T51) or the titin-binding protein myomesin. One of the beads, attached to a micropipet, was used to stretch the molecule, while the other bead, captured in an optical trap, was used to measure the force developed upon stretch. The force-length relations revealed that titin can be stretched up to a length of ~6 μm, reaching forces of ~100 pN. When the length of the molecule was held constant following a rapid stretch, the force decreased logarithmically, resembling the process of stress relaxation in muscle.

M-AM-A8

EXTENSIBILITY OF TITIN VISUALIZED BY ELECTRON MICROSCOPY OF SHADOWED MOLECULES.

((**L. Tskhovrebova** and J. Trinick)) Veterinary School, Bristol University, Langford, Bristol BS18 7DY, UK.

The molecular mechanism of titin elasticity is not known. The molecule consists mainly of immunoglobulin (Ig)- and fibronectin (FN)-like domains, but in the I-band there is a small region of unknown structure high in P, E, V and K residues. It has been proposed that extension involves reversible unfolding of Ig-like domains or the PEVK-region.

Isolated molecules are very flexible but striking images of straightened and uni-directionally oriented strands can be seen in the electron microscope after drying from thin layers of glycerol-containing buffers.

This "molecular combing" results from: (a) preferential attachment of the ends of the molecules to the mica substrate (probably due to electrostatic interaction between the positively charged ends of the molecule and negatively charged mica), and (b) the surface tension force acting at the receding solvent meniscus. This force is $F = \gamma\pi D$ ~800 pN, assuming γ = 64 dyne/cm is the solvent-air surface tension and a titin diameter of 4 nm.

Analysis of the micrographs, together with length estimates based on sequence, indicates that: (a) a commonly observed ~1 micron long strand is probably the conserved (M-line to PEVK) segment of the molecule; (b) intact molecules can separate under tension into conserved and N-terminal (PEVK to Z-line) segments at or near the PEVK region; (c) separation of the conserved and N-terminal segments appears to result from local unfolding of the PEVK region.

Although, the PEVK region seems to be more compliant than the rest of the molecule, 10-50% extension was also seen in the conserved segment.

M-AM-A9

BIOMIMETIC MODEL COMPOUNDS USED TO DEFINE THE COORDINATION GEOMETRY OF THE VANADATE (Vi) CENTERS IN Me^{2+}Vi-S1 AND Me^{2+}ADPVi-S1 COMPLEXES

((K. Ajtai[1], F. Dai[1], S. Park[1], C. R. Zayas[1], Y. M. Peyser[2], A. Muhlrad[2] and T. P. Burghardt[1])) [1]Mayo Foundation, Rochester, MN 55905, USA and [2]Hebrew University, Jerusalem 91120, Israel

The CD spectrum was measured from known Vi esters of chiral vicinal diols, hydroxycarboxylates and cyclodextrins. Vanadium 51 (^{51}V) NMR studies define the coordination geometry of the model Vi centers in solution so that CD signals characteristic to trigonal bipyramidal and octahedral coordination geometries were identified. The CD spectrum was also measured from Me^{2+}Vi bound to S1 (Me^{2+}Vi-S1) and Me^{2+}ADPVi trapped Sl (Me^{2+}ADPVi-S1) and a comparison was made between the model and protein spectra to determine the coordination geometry of the protein bound Vi center. The comparison of the CD signal characteristics suggests that the S1 binds Me^{2+}Vi with the trigonal bipyramidal geometry while the S1 binds Me^{2+}ADPVi with octahedral geometry in the Vi center. These results show a possible difference in Vi geometry in the ATP binding site between the rabbit myosin S1 obtained in solution and the Dictyostelium myosin motor domain obtained from crystallography[3]. This work was supported by NIH R01 AR 39288, AHA 930 06610 and the Mayo Foundation.

(3) Smith and Rayment, Biochemistry 35:5404, 1996.

M-AM-B1

CRITICAL PORE RESIDUES INVOLVED IN μ-CTX BINDING TO THE RAT SKELETAL MUSCLE SODIUM CHANNEL REVEALED BY SINGLE CYSTEINE MUTAGENESIS

((**Ronald A. Li**, Robert G. Tsushima, Peter H. Backx)) Dept. of Medicine, University of Toronto, Toronto, Canada. (Sponsored by M. Silverman)

We have studied the block of the rat skeletal muscle sodium channel (rSkm1) by μ-conotoxin (μ-CTX) in which single amino acids within the pore (P-loop) were substituted by a cysteine. Among 17 single cysteine mutants studied, 5 were significantly different from the wild type rSkM1 channel (IC_{50}=17.5±2.8 nM). E758C and D1241C were less sensitive to μ-CTX block (IC_{50}=220±39 nM and 112±24 nM respectively) whereas the tryptophan mutants W402C, W1239C, and W1531C showed enhanced μ-CTX sensitivity (IC_{50}= 1.9±0.1, 4.9±0.9 and 5.5±0.4 nM respectively). Application of the negatively-charged sulfhydryl reactive compund, MTSES, enhanced the toxin sensitivity of D1241C (IC_{50}=46.3±12 nM) but had no effect on E758C mutant channels (IC_{50}=199.8±21.8 nM). On the other hand, the positively charged MTSEA completely abolished the μ-CTX sensitivity of E758C (IC_{50}> 1μM) while increasing the IC_{50} of D1241C to 334±103 nM. Modification of the tryptophan mutants with MTSEA and MTSES also changed the IC_{50} for μ-CTX block (W402C: 12.5±1.2 after MTSEA, 7.1±1.3 nM after MTSES; W1239C: 15.1±1.9 nM after MTSEA, 8.2±0.5 nM after MTSES; W1531C: 12.2±3.4 nM after MTSEA, 11.8±3.1 nM after MTSES), suggesting that the bulkiness of the tryptophan's indole group is important in determining the toxin affinity. Our results therefore establish that the negative charges of E758 and D1241 are important for interacting with the toxin binding domain of μ-conotoxin and further suggest that the trytophan residues within the pore in domain I, III and IV influence μ-CTX binding.

M-AM-B2

HIGHLY CONSERVED RESIDUES IN THE S3 SEGMENTS OF RAT SKELETAL MUSCLE SODIUM CHANNELS PLAY A ROLE IN CHANNEL ACTIVATION AND INACTIVATION

((**Ronald A. Li**, Robert G. Tsushima, Peter H. Backx)) Dept. of Medicine, University of Toronto, Toronto, Canada.

Aspartates (i.e. D197, D640, D1094 and D1413) and phenylalanines (i.e. F198, F639, F1095 and F1412) found in the third transmembrane segment of all 4 domains of the Na channel are absolutely conserved residues among different Na and Ca channel isoforms and are highly conserved in other voltage-gated channels. These S3 Asp residues have been proposed to form salt bridges with the voltage sensor in S4 and hence are expected to influence channel activation. However, the disease equine hyperkalemic periodic paralysis (HPP) involving the mutation of one of the four Phe residues (i.e. F1412L) of the Na channel is known to disrupt inactivation. We therefore examined the roles of these residues in Na channel activation and inactivation using single cysteine mutagenesis and expression of the mutant channels into *Xenopus* oocytes. All the D mutants studied but none of the F mutants displayed rightward shifts in steady-state activation curves by 5 to 15 mV. Some of these D mutations also altered channel inactivation: increased time-to-peak current (D640C and D1413C), slowed rates of whole cell current decay (D1413C), leftward (D640C) and rightward (D197C and D1413C) shifts in the steady-state inactivation curve and slowed rates of recovery from inactivation (D197C, D640C and D1413C). Remarkably, the rate of entry into the inactivated state of D1413C, as reflected by the rate of whole-cell current decay, was slowed while the time required for total recovery from inactivation was prolonged (5-fold), suggesting that this residue is critical for coupling inactivation to activation. Among 4 of the Phe residues studied, only F1412C displayed significant changes in inactivation: increase in sustained current, faster recovery from inactivation and rightward shifts of the steady-state inactivation curve. These results therefore suggest that these highly conserved residues in S3 of all the four domains play a role in channel activation and inactivation.

M-AM-B3

FUNCTIONAL AND STRUCTURAL STUDIES OF S4-S45 SEGMENTS. IMPLICATION FOR THE SODIUM CHANNEL ASYMMETRY.

((O. Helluin and **H. Duclohier**)). URA 500 CNRS-Univ. Rouen (IFRMP 23), 76821 Mont-Saint-Aignan, France.

Past and recent studies point out S4 segments as the main sensors of voltage-gated ion channels. To assay sequence specificity of the four homologous S4-S45 fragments, characterized especially by one proline residue at different positions (domains I-III) and its absence in domain IV, these chemically-synthesized peptides were reconstituted into planar lipid bilayer. Investigation of secondary structures was followed with circular dichroism in media of different polarity. Despite a reduced number of positive charges, segments S4-S45(I-III) - with proline- are more voltage-dependent than S4-S45(IV). Domain III shows the greatest V_e (6 ± 2 mV) while S4-S45 of domains I and II sharing a proline at another position display a similar voltage-sensitivity (V_e = 8.5 ± 3 mV). The mean number per aggregate ranging from 4 to 6 is another experimental support (see e.g. Papazian et al., Neuron 14:1293-1301) that S4s could drive the proper channel folding. Highest voltage-dependence is correlated to the largest conformational transition (α→extended) mainly involving the S45 moiety (Helluin et al., Biochim. Biophys. Acta 1279:1-4) when the environment becomes hydrophilic instead of hydrophobic. These data support recent kinetic models as the "series-parallel" scheme (Keynes, Quater. Rev. Biophys. 27:339-434) where S4s actions are not equivalent.

Supported by GdR 1153 CNRS and by the C.E.B. (Rouen, Normandie).

M-AM-B4

COMPLEX GATING CHANGES CAUSED BY THE KPQ DELETION IN THE III-IV LINKER OF HUMAN HEART Na^+ CHANNEL.

((**T. Nagatomo**, Z. Fan, B. Ye, #G.S. Tomkavich, C.T. January, #J.W. Kyle and J.C. Makielski)) Univ. of Wisconsin, Madison, WI, and #Univ. of Chicago, Chicago, IL.

We compared the kinetic characterization of a human heart voltage-gated Na^+ channel α-subunit (hH1a) mutant associated with long-QT syndrome, a KPQ deletion at 1505-1507 (ΔKPQ), with wild type (WT). Previous reports of kinetics in oocytes (Bennett PB et al, 1995) and in transfected cells (An R-H et al, 1996) are discrepant. cDNA encoding either wild type or ΔKPQ mutant of hH1a were stably transfected into a mammalian cell line (HEK293). Na^+ currents (I_{Na}) were recorded using the whole-cell patch-clamp technique. Time to peak I_{Na} and decay of I_{Na} were more rapid in KPQ at -40 mV, but no different at 0 mV. Recovery at -120 mV was more rapid for KPQ. Steady-state inactivation midpoint was slightly more negative and the slope factor was increased for ΔKPQ (WT: $V_{1/2}$=-90.7±1.1, κ=5.5±0.15, n=8; KPQ: *$V_{1/2}$=-93.5±0.64, *κ=6.9±0.12, n=9). Activation midpoint was more positive for ΔKPQ (WT: $V_{1/2}$=-43.9±1.0, κ=-7.6±0.64, n=6; KPQ: *$V_{1/2}$=-37.3±1.9, κ=-8.6±0.12, n=5). Persistent I_{Na} detected at 240 ms was greater for ΔKPQ (WT: 0.14±0.02 %, n=8; ΔKPQ: *0.58±0.05 %, n=6, of peak value) but less than previous reports. ΔKPQ produces complex effects on voltage-dependent kinetics; the electrophysiological phenotype may depend upon details of the preparation and protocol. (* $p < 0.05$)

M-AM-B5

STABILIZATION OF INACTIVATION BY LIDOCAINE UNDERLIES PREFERENTIAL BLOCK OF LATE CURRENT IN THE LONG-QT MUTANT Na^+ CHANNELS.

((R. Dumaine and G. E. Kirsch)) Rammelkamp Center, MetroHealth campus, CWRU School of Medicine, Cleveland OH 44109.

Inherited long-QT syndrome is associated with delayed ventricular repolarization, syncope and the risk of sudden death. The chromosome 3-linked form of the disease (LQT3) is associated with two point mutations (substitutions N1325S and R1644H), and a deletion of residues 1505 to 1507 (ΔKPQ) in the sodium channel α-subunit. These mutations potentiate non-inactivating, late inward currents that may be responsible for delayed repolarization. The late currents are generated by dispersed reopenings (R/H and N/S) or by reopenings combined with prolonged bursting (ΔKPQ). Since the underlying mechanisms of the late current varied we tested whether lidocaine, a class Ib antiarrhythmic drug, blocks all LQTS mutant Na channels in a similar manner. Mutant channels were expressed in *Xenopus* oocytes and electrophysiological measurements were made using whole cell and patch clamp techniques. Lidocaine preferentially blocked late current over peak current in all the channels. But, contrary to expectation, lidocaine was equally effective in blocking late current in all three channels. At the single channel level lidocaine reduced the occurrence of both dispersed reopenings and burst activity without changing the open gating parameters. Inactivating prepulses in the absence of drug selectively reduced the occurrence of bursting without affecting dispersed openings. These results suggest that lidocaine block of the late current in all three LQTS mutant Na channels acts via a common mechanism involving stabilization of the inactivation. We therefore expect lidocaine to be effective for all three biophysical phenotypes of LQT3 in a long QT normalization therapy.

M-AM-B6

MEMBRANE VOLTAGE DETERMINES LOCAL ANESTHETIC AFFINITIES OF CLONED NA CHANNELS.

((1S.N. **Wright**, 2S.-Y. Wang, 3R.G. Kallen and 1G.K. Wang)) 1Brigham & Women's Hospital, Harvard Medical School, Boston, MA 02115; 2SUNY, Albany, NY 12222; 3University of Pennsylvania School of Medicine, Philadelphia, PA 19104 (Spon. by G.K.W.)

We transiently expressed cloned Na channels from human heart muscle (hH1) and rat skeletal muscle (μ1) in HEK 293t cells to investigate voltage-dependent binding of the tertiary amine local anesthetics (LAs) cocaine and lidocaine. Under whole-cell voltage-clamp conditions, we delivered 10 sec conditioning pulses of various amplitudes to allow LA binding to reach steady state. A gap of 100 ms at the holding potential (-140 mV) after the conditioning pulses allowed drug-free channels to recover from fast inactivation. We then delivered a test pulse to assess the percentage of Na current blocked by either cocaine or lidocaine. We found that blockade of the Na current at hH1 and μ1 channels saturated at -180 to -160 mV (weak block) and at -80 to -70 mV (strong block) and that block increased gradually as the amplitude of the conditioning pulse became less negative. This finding suggested that these LAs bind primarily with either resting or inactivated channels and that as the proportion of inactivated channels increased (at less negative potentials), block also increased. At negative voltages (-180 to -160 mV), the affinities of resting hH1 and μ1 channels for cocaine, as well as for lidocaine, were the same. The LA affinities of these Na channel isoforms diverged at about -120 mV, with hH1 channels having the higher affinity. At -70 mV, the affinities of inactivated hH1 and μ1 channels for cocaine were the same, whereas hH1 channels had a 2-fold higher affinity than μ1 channels for lidocaine. At -100 mV, hH1 channels had an approximately 10-fold higher affinity than μ1 channels for either cocaine or lidocaine. Our findings indicate that the higher affinity of the hH1 isoform for these LAs at normal resting potentials is due to stronger voltage-dependent modulation of affinity, rather than to a higher intrinsic LA receptor affinity.

M-AM-B7

STATE-DEPENDENT MODULATION OF SODIUM CHANNEL ACTIVATION BY A ß-SCORPION TOXIN FROM *TITYUS DISCREPANS* VENOM. ((**Robert G. Tsushima**, Adolfo Borges*, Peter H. Backx)) Dept. of Medicine, Physiology and Clinical Biochemistry*, University of Toronto, Toronto, Canada.

Scorpion toxins have provided a useful tool for the examination of the structure and biophysical properties of ion channels. We have examined the effects of a ß-scorpion toxin purified from the venom of the Venezuelan scorpion *Tityus discrepans* (TdTX) on the rat skeletal muscle Na channel (rSkM1) coexpressed with the rat brain $ß_1$ subunit in *Xenopus* oocytes. Na currents were evoked by step depolarizations from -80 to +50 mV (V_{hold} -120mV) at 0.3 Hz. Activation curves for were fit to single Boltzmann distributions ($V_{½}$= -22.5±0.5 mV; 4.5±0.1 e_m, n=4). TdTX (100 nM, n=4) produced a leftward shift in the voltage dependence of activation such that activation curves were best fit to double Boltzmann distributions with $V_{½}$ of -21.4±0.5 mV (5.0±0.7 e_a) and -47.7±1.3 mV (8.9±0.9 e_a) (42. 6 ± 3.8%). TdTX reduced peak Na conductance by 32.6 ± 4.8% but had no pronounced effect on current inactivation. Similar changes were observed in the absence of the $ß_1$ subunit suggesting that modulation does not involve the $ß_1$ subunit. TdTX modification of the rSkM1 could be augmented by increasing the rate of stimulation (enhanced use dependence) or by introducing conditioning depolarized pulses prior to the test pulse. The conditioning pulse modification was voltage- and duration-dependent. Prolongation of the conditioning pulse duration from 2 to 50 ms enhanced channel modification. The latter effect suggests that TdTX preferentially binds to the inactivated state of the Na channel. We studied this hypothesis by examining the effects of TdTX on the fast-inactivation deficient mutant, IFM/QQQ. TdTX produced little or no shift in the activation of the IFM/QQQ channel although there was an 18.0±4.0% reduction in Na conductance, suggesting that the alteration in channel activation by TdTX is enhanced by inactivated-state binding. These results indicate modulation of rSkM1 channel gating by ß-scorpion toxins involves preferential binding to the inactivated state of the α subunit of the Na channel and does not require the presence of the $ß_1$ subunit.

M-AM-B8

LIDOCAINE INDUCES PHASIC BLOCK OF A MUTANT SKELETAL MUSCLE NA^+ CHANNEL LACKING FAST INACTIVATION. ((**K.J. Gingrich** and L.Wagner II)) Depts. of Anes., Pharm. and Phys., U. of Rochester, School of Medicine, Rochester, NY 14642

Fast inactivation is required for phasic block by local anesthetics in heart (Bennett *et al*, 1995) while slow inactivation is involved in skeletal muscle (Balser *et al*, 1996). To examine the role of fast inactivation in skeletal muscle we studied the effects of lidocaine on wild type (WT) rat skeletal muscle α-subunit (rskm-µ1) Na^+ channel coexpressed with the β-subunit and a mutant form (I1303Q, F1304Q, M1305Q) that lacks fast inactivation (QQQ). *Xenopus* oocytes were injected with cRNA and Na^+ currents (*I*) were measured using two-electrode voltage clamp.

To assess phasic block (PB) we employed a pulse train protocol (fifteen 20ms depolarizations [-10mV] at 15Hz, HP = -100mV) and calculated the ratio of the peak *I* for last pulse (#15) and first pulse (I_{15}/I_1). Grouped data are means±SEM, N≥5. Fig. A shows superimposed, typical responses from three pulses, as indicated, from an oocyte expressing WT. I_{15}/I_1 is reduced slightly (0.93±0.01) likely reflecting accumulation of inactivation. 1mM lidocaine (LDCN) reduces I_1 through tonic block, but also induces significant PB (I_{15}/I_1 = 0.23±0.02). Fig. B shows control responses for QQQ and demonstrates the absence of fast inactivation. LDCN depression of I_1 is similar to WT but is accompanied by current decay consistent with open channel block. Interestingly, PB is observed but is two-fold less than WT (I_{15}/I_1= 0.64±0.03). These results indicate that elimination of fast inactivation in rskm-µ1 impairs but does not abolish PB. Furthermore, they suggest the involvement of open channel interactions in long-lived local anesthetic block of skeletal Na^+ channel isoforms.

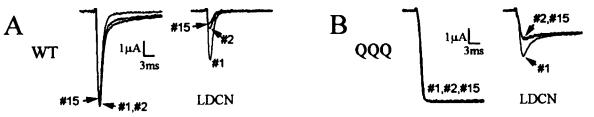

M-AM-B9

ON THE ALLOSTERIC MODULATION OF NEUROTOXIN BINDING ON VOLTAGE-GATED SODIUM CHANNELS

((**Dalia Gordon** and Sandrine Cestèle)) Faculty of Medicine Nord, Biochemistry, Bd. Pierre Dramard, 13916 Marseille, France.

Voltage-gated sodium channels serve as targets for may neurotoxins, that bind to several distinct but allosterically interacting receptor sites. Using the potential-sensitive high affinity binding of the scorpion α-toxin AaH II to rat brain synaptosomes as probe for conformational changes induced on sodium channels by binding of veratridine, brevetoxin and tetrodotoxin (TTX), we suggest that depolarization-induced conformational changes differentially modulate the effects of each of the neurotoxins on AaH II binding: the enhancement by TTX is independent of depolarization while that by veratridine is potentiated. Brevetoxin inhibitory effect is reduced by increasing membrane depolarization. Both TTX and veratridine reverse the inhibition of AaH II binding by brevetoxin at resting membrane potential, but at 0 mV only veratridine effect is increased by brevetoxin. On the basis of a conformational state model, we suggest that simultaneous neurotoxin binding may (1) stabilize different channel open states and (2) cause uncoupling between functional state stabilization and additional alteration of the channel structure, that provide explanation to asymmetric cooperativity in toxin effects at different membrane potentials. Our study contribute to the clarification of the dynamic conformational changes induced on the sodium channel protein in the process of gating and allosteric modulation by simultaneous neurotoxins occupancy of distinct receptor sites.

ANION CHANNELS

M-AM-C1

BOTH pI_{ClN} AND CLC-6 ACTIVATE I_{ClN}, AN ENDOGENOUS CHLORIDE CURRENT IN *XENOPUS* OOCYTES, WHICH DIFFERS FROM $I_{Cl,SWELL}$

((**J. Eggermont**, J. Tytgat, G. Buyse, T. Voets, G. Droogmans, B. Nilius)) Laboratorium voor Fysiologie, K.U.Leuven, Campus Gasthuisberg, B-3000 Leuven, Belgium

pI_{ClN} is a protein that induces an outwardly-rectifying, nucleotide-sensitive chloride current (I_{ClN}) when expressed in *Xenopus* oocytes. Phenotypical similarities between I_{ClN} and $I_{Cl,swell}$ have led to models in which pI_{ClN} functions either as the volume-sensitive chloride channel or as a cytosolic regulator thereof.
A systematic comparison between I_{ClN} and $I_{Cl,swell}$ in *Xenopus* oocytes revealed significant differences in anion selectivity, inactivation kinetics, degree of rectification, sensitivity to changes in extracellular osmolarity and pharmacology. The I_{ClN} current was also detected in 6.2% of non-injected control oocytes. Interestingly, a chloride current completely identical to I_{ClN} could also be observed when oocytes were injected with RNAs coding for different splice variants of human ClC-6. We therefore conclude that I_{ClN} corresponds to an endogenous chloride conductance in *Xenopus* oocytes which can be activated by expression of foreign proteins such as pI_{ClN} and ClC-6 isoforms and which clearly differs from the endogenous volume-activated chloride channel. In addition, the subcellular localization of pI_{ClN} in mammalian endothelial cells was studied using cellular fractionation or fluorescence confocal microscopy. The majority of pI_{ClN} was recovered in the cytosolic fraction, but a small fraction of pI_{ClN} copurified with the microsomal fraction. However, confocal microscopy did not reveal a plasma membrane location for pI_{ClN}. Furthermore, the distribution of pI_{ClN} did not change when the cells were subjected to extracellular hypotonicity. It is therefore unlikely that pI_{ClN} forms a plasma-membrane located anion channel responsible for $I_{Cl,swell}$

M-AM-C2

THE VOLUME SET-POINT OF A SWELLING-ACTIVATED ANION CHANNEL IS MODULATED BY INTRACELLULAR ELECTROLYTES. ((F. Emma, M. McManus and K. Strange)) Children's Hospital, Boston, MA 02115. (Spon. by E. Delpire)

A swelling-activated, outwardly rectifying anion channel termed VSOAC (volume-sensitive organic osmolyte/anion channel) is observed ubiquitously in mammalian cells and is the major pathway for organic osmolyte efflux. Patch clamp measurements in C6 glioma cells revealed that channel activation is sensitive to intracellular electrolyte levels. With high (135 mM CsCl) versus low (45 mM CsCl) salt concentration in the patch pipette solution, VSOAC current activation was slower (1-2 pA/pF/min versus 14 pA/pF/min) and required much greater cell swelling (>80% versus ~30%) before it could be detected. These findings suggest that the volume sensitivity of the channel is controlled by cytoplasmic inorganic ion concentrations. Whole cell patch clamp measurements may not reflect adequately normal physiological functions, however. In order to determine whether cellular electrolytes alter VSOAC activity in intact cells, we acclimated C6 cells to hypertonic medium. Hypertonic shrinkage was followed by a rapid regulatory volume increase mediated by Na^+, K^+, and Cl^- accumulation. Electrolytes were replaced slowly by the organic osmolyte *myo*-inositol during prolonged exposure to hypertonicity. The degree of swelling-induced VSOAC activation (measured as ^{3}H-taurine efflux) was correlated directly with time of exposure to hypertonicity and inversely correlated (r=0.98) with measured intracellular Na^+, K^+ and Cl^- levels. Measurement of ^{3}H-taurine efflux in response to a range of volume perturbations in cells with high or normal inorganic ion concentrations revealed that high electrolyte levels increase channel volume set point. Modulation of VSOAC volume sensitivity by inorganic ions allows cells to selectively utilize electrolytes or a combination of electrolytes and organic osmolytes for volume regulation after swelling. Control over the type of solute used for volume regulation is advantageous, allowing cells to control intracellular ionic composition and prevent increases in cytoplasmic ionic strength during volume regulation.

M-AM-C3

I_{Cln} BINDS SELECTIVELY TO MYOSIN LIGHT CHAIN AND A PROTEIN KINASE. ((R. Sanchez-Olea, M. Coghlan and K. Strange)) Children's Hospital, Boston, MA, 02115. (Spon. by R.J. Turner)

VSOAC is a swelling-activated anion channel responsible for volume regulatory Cl and organic solute efflux. A substantial body of evidence suggests that the protein I_{Cln} (Paulmichl et al. *Nature* 356:238, 1992) is either the VSOAC channel or a channel regulator. In an overall effort to define the function of I_{Cln}, we have begun to identify and characterize proteins that bind to and interact with this molecule. Immunoprecipitation of ^{35}S-labeled C6 glioma cell lysates with polyclonal anti-I_{Cln} antiserum or treatment with an I_{Cln} affinity resin revealed that I_{Cln} binds selectively to several cellular proteins. Microsequencing demonstrated that the 17 kDa binding protein is the non-muscle isoform of myosin light chain (MLC). I_{Cln} has consensus sequences for phosphorylation by PKA, PKC, PKG, casein kinase I (CKI) and II (CKII) and tyrosine kinases. Immunoprecipitation of lysates from $^{32}PO_4$-labeled C6 glioma cells demonstrated that I_{Cln} is constitutively phosphorylated *in vivo*. I_{Cln} is phosphorylated when ^{32}P-ATP is added to affinity isolates or immunoprecipitates. Phosphorylation is prevented when binding proteins are competed off the resin by treatment with excess free I_{Cln}. These findings demonstrate that a protein kinase binds selectively to I_{Cln}. The I_{Cln} associated kinase has broad substrate specificity and is inhibited by heparin, DRB and zinc in a concentration-dependent manner. Phosphoamino acid analysis demonstrated that this kinase is a serine/threonine kinase. Western analyses and functional assays ruled out the possibility that the I_{Cln} associated kinase is either CKI or CKII. In gel kinase assays suggest that the catalytic component of the I_{Cln} associated kinase is an ~40 kDa protein. These results indicate that I_{Cln} associates tightly with a protein kinase *in vivo* and suggest that phosphorylation may play an important role in modulating I_{Cln} function. Association of I_{Cln} with MLC may play a role in the transduction of cell swelling into anion channel activation.

M-AM-C4

BARRIER MODELS FOR WILD-TYPE AND MUTANT CFTR CHLORIDE CHANNELS. ((**Paul Linsdell** and John W. Hanrahan)) Department of Physiology, McGill University, Montréal, Québec, Canada.

Voltage dependent block of the CFTR chloride channel by intracellular gluconate ions was used to develop both 3-barrier, 2-site and 4-barrier, 3-site multi-occupancy energy barrier profiles for the channel permeation pathway. Both models were able to reproduce Cl permeation and gluconate block measured using single channel recording under a number of different sets of ionic conditions, including the reduction in gluconate affinity due to increasing extracellular Cl concentration, a manifestation of multi-ion pore behaviour. Barrier models also replicated the dependence of channel conductance on symmetrical Cl concentration. The 3 site model could be further modified to reproduce the previous evidence that CFTR is a multi-ion pore, the anomalous mole fraction dependence of channel conductance seen in Cl/SCN mixtures. Specific modifications of this model near the cytoplasmic end of the pore were able to reproduce the loss of anomalous mole fraction behaviour and reduction in Cl and SCN conductance seen in the pore mutant R347D-CFTR. This 3 site model is therefore able to reproduce all of the available data that CFTR is a multi-ion pore, and may allow some correlation between theoretical and physical sites in the channel pore. *Supported by the Canadian CF Foundation, MRC (Canada) and NIH(NIDDK).*

M-AM-C5

LYSOPHOSPHATIDYLGLYCEROL-A NOVEL EFFECTIVE DETERGENT FOR SOLUBILIZING AND PURIFYING THE CFTR. ((**Pingbo Huang**, Qiyi Liu, and Gene A. Scarborough)) Dept. of Pharmacology, Univ. of North Carolina, Chapel Hill, NC 27599

Similar to the CFTR expressed in Sf9 insect cells, unglycosylated CFTR expressed in yeast is not effectively solubilized by a variety of commonly used detergents, requiring instead harsh alkali and SDS treatments, which would denature most proteins. We report here that the mild detergent, lysophosphatidylglycerol (LPG), is a very effective detergent for solubilizing the CFTR expressed in both yeast and Sf9 insect cells. LPG solubilizes nearly 100% of the CFTR in yeast in the absence of NaCl, and none in the presence of 1M NaCl. It is also very potent in preventing aggregation of the CFTR during subsequent purification. Exploiting these characteristics, a rapid simple procedure for the purification of functional CFTR expressed in yeast has been developed. It includes selective solubilization in the presence and absence of NaCl followed by nickel-chelate chromatography of His-tagged CFTR. The CFTR produced by this procedure is 90% pure. Purified CFTR molecules were reconstituted into planar lipid bilayers for single channel recording. The reconstituted CFTR exhibits regulatory chloride channel activities with a slope conductance of 7.1 pS and a reversal potential of -32 mV (cis:trans = 300:50). The effectiveness and simplicity of this new CFTR purification procedure should greatly facilitate a variety of biochemical and biophysical studies of this important protein. Furthermore, the potency of LPG in solubilizing the notoriously intractable unglycosylated CFTR suggests that it may be useful for solubilizing other difficult membrane proteins as well.

M-AM-C6

EACH SUBUNIT FORMS AN INDEPENDENT PORE IN THE DIMERIC CLC-0 CHLORIDE CHANNEL
((**Uwe Ludewig**, Michael Pusch & Thomas J. Jentsch)) ZMNH, Hamburg University, Martinistr. 52, D-20246 Hamburg, Germany

The *Torpedo* chloride channel ClC-0 is the prototype of a large gene family of chloride channels which have roles in transepithelial transport and in regulating electrical excitability and cell volume. ClC-0 is well known as a "double barrelled" channel with two identical conductance levels of ~8pS. A mutant channel (S123T) has reduced conductance, altered current-voltage rectification, is less selective between different anions and "fast" gating is slower, but shows a similar "double barrelled" behaviour. By using concatamers of wild type and mutant subunits we show that different subunits can associate to form heteromeric channels. In such channels we find two pores, one with conductance and ion selectivity similar to a single wild type pore and one resembling the characteristics of a mutant pore. In coexpression experiments we only observed pores with wild type and mutant characteristcs, but never pores with intermediate properties. Thus, our results favour a dimeric structure of CLC-0. In a concatamer of mutant S123T with another mutant (K519E, a more carboxy-terminally located mutation with characteristics similar to S123T; Pusch et al., Nature, 373:521f, 1995), we find S123T and K519E like pores, but no wild type pores. Thus, both different protein regions of a single subunit contribute to a single pore, suggesting that each pore is formed by a single subunit. In addition, by constructing open dwell time histograms for each pore, we find that both pores are gated independently from the physically attached pore. By contrast, slow gating that is simultaneously operating on both pores is a function of both subunits of the dimeric channel.

M-AM-C7

A MUTATION IN THE HUMAN MUSCLE CHLORIDE CHANNEL THAT CAUSES PROFOUND EFFECTS ON PERMEATION ((**Ch. Fahlke**, C. L. Beck, and A. L. George, Jr.)) Vanderbilt University, Nashville, TN 37232

Autosomal dominant myotonia congenita is an inherited disorder of skeletal muscle caused by mutations in a voltage-gated Cl^- channel gene (*CLCN1*, 7q35). Here, we report that a mutation predicting the substitution of glycine-230 by glutamic acid (G230E) between segments D3 and D4 dramatically alters the pore properties of a recombinant human muscle Cl^- channel (hClC-1) when expressed in a mammalian cell line (tsA201) and examined by whole-cell recording. Only slight effects on gating leading to an increase of the relative open probability at the resting potential of skeletal muscle, but dramatic effects on specific pore properties of the mutant were observed. The cation to anion permeability ratio of the mutant was greatly increased resulting in a $P_{Na,K}/P_{Cl}$ of 0.25. Whereas wild-type (WT) channels are characterized by pronounced inward rectification of the I-V relationship and a $Cl > SCN > Br > NO_3 > I > CH_3SO_3$ selectivity, G230E shows outward rectification at positive potentials and a $SCN > NO_3 > I > Br > Cl > CH_3SO_3$ selectivity. The ion conduction pathway of hClC-1 is characterized by two different high affinity binding sites for iodide. These binding sites are preserved in the mutant pore but have decreased affinities for iodide. These findings fit well with the idea that glycine-230 is located at the entrance of the hClC-1 ion pore; introduction of a negative charge at this position decreases the anion flux, weakens the interaction with blocking anions, and may provide a binding site for cations.

M-AM-C8

A QUEST FOR A SOLUBLE DOMAIN OF AN ION CHANNEL
((**M. Maduke** and C. Miller)) HHMI, Brandeis University, Waltham, MA 02254

Our understanding of the molecular structure of membrane proteins has been limited by the difficulty of obtaining 3-dimensional crystals. In some cases, this difficulty has been circumvented partially by crystallization of soluble domains of membrane proteins. This approach has not yet been successful for ion channels, though ion channels ostensibly contain structurally interesting soluble domains. To identify potential domains, a split-channel strategy was developed and applied to ClC-0, a well-characterized member of the ClC family of chloride channels. The current topology model for this family places the last 230 (of 805) amino acids on the cytoplasmic side of the membrane. To test for the existence of an independent folding domain within this region, several split channels were constructed, and cRNAs corresponding to the N- and C-terminal parts of the protein were injected into *Xenopus laevis* oocytes. Neither the N-terminal (which contained all 12 putative transmembrane domains) nor the C-terminal RNAs alone induced expression of current. When coinjected, however, some of the pairs induced current indistinguishable from that of wild-type ClC-0. Thus, the independently produced C-terminal protein folded correctly and associated with the N-terminal protein to form functional channel. To test directly the ability of the C-terminal protein to behave as a soluble domain, it was overexpressed in *E. coli*, purified through use of a His tag, and injected into oocytes. The purified protein reconstituted ClC-0 channel activity in oocytes that had been injected with the N-terminal RNA, thus behaving as an independent and functionally essential domain of a chloride channel.

M-AM-D1

HYDRATION OF PYRIMIDINE/PURINE/PYRIMIDINE DNA TRIPLE HELICES AS REVEALED BY FT-IR SPECTROSCOPY: A ROLE OF CYTOSINE METHYLATION. ((L.-S. Kan[a], Y. Fang[b], S.-B. Lin[c], Y. Wei[b], C. Bai[b], Y. Tang[b])) [a]Institute of Chemistry, Academia Sinica, Taipei, Taiwan. [b]Institute of Chemistry, Academia Sinica, Beijing, China. [c]Graduate Institute of Medical Technology, National Taiwan University, Taipei, Taiwan.

Hydration of pyrimidine/purine/pyrimidine DNA hairpin triplex was studied by a comparison of triplex (CC·AG6) formed by a host oligodeoxy-pyrimidine of 5'-d$(TC)_3T_4(CT)_3$ (CC) with a target hexadeoxypurine 5'-d$(AG)_3$ (AG6) strand and by triplexes (MM·AG6, MC·AG6, and CM·AG6) formed by oligonucleotides with the exact sequences as above except 5-methylcytosine replaced all (MM), 5' end half (MC), and 3' end half (CM) cytosine bases in CC via FT-IR spectroscopy in hydrated film. Results revealed that: (1) all these triplexes have a similar hydration pattern. (2) In the CC·AG6 triplex the S-type sugars are always dominant in all hydration states, whereas in MM·AG6 triplex the relative population of the N-type sugars is very close to that of the S-type between 86% and 66% of hydration. Furthermore, the sugar conformation in two partially modified triplexes (CM·AG6, and MC·AG6) are dominant by the N-type at lower humidities. (3) The effect of introducing a methyl group on cytosine is to generate a spine of hydrophobic region in MM (MC and MC). The enlarging hydrophobic area not only increase the stability in solution, and also the stability in sodium hydration films of the pyrimidine/purine/pyrimidine hairpin triplexes.

M-AM-D2

A COMPUTATIONAL APPROACH FOR MODELING NUCLEIC ACID HAIRPIN STRUCTURE. ((C.-S. Tung)) Theoretical Biology and Biophysics, Los Alamos National Laboratory, Los Alamos, NM 87545.

Hairpin is a structural motif frequently observed in both RNA and DNA molecules. This motif is involved specifically in various biological functions (e.g., gene expression and regulation). In order to understand how these hairpin motifs perform their functions, it is important to study their structures. Compared to protein structural motifs, structures of nucleic acid hairpins are less known. Based on a set of reduced coordinates for describing nucleic acid structures and a sampling algorithm that equilibrates structures using Metropolis Monte Carlo simulation, we developed a method to model nucleic acid hairpin structures. This method was used to predict the structure of a DNA hairpin with a single nucleotide loop. The lowest energy structure from the ensemble of 200 sampled structures has a RMSD of < 1.5 Å from the structure determined using NMR. Additional constraints for the loop bases were introduced for the modeling of an RNA hairpin with two nucleotides in the loop. The modeled structure of this RNA hairpin has extensive base stacking and an extra hydrogen bond (between the CYT in the loop and a phosphate oxygen) as observed in the NMR structure.

M-AM-D3

STRUCTURE, FUNCTION, AND EVOLUTION OF THE VIRUS INTERNAL RIBOSOME ENTRY SITES. ((S.-Y. Le and J.V. Maizel, Jr.)) LMMB, DBS, NCI, NIH, Frederick MD 21702.

The translational control involving internal ribosome binding occurs in the picornavirus, hepatitis C virus (HCV), and pestivirus. Internal ribosome binding utilizes cis-acting genetic elements of approximately 450 and 320 nucleotides (nt) termed the internal ribosome entry sites (IRES) found in the 5'-untranslated region (5'UTR) of picornaviruses and HCV respectively. Although these IRES elements are quite different in their primary sequence, a similar folding structure with a conserved 3' structural core in the IRES. Phylogenetic analysis and RNA folding of these virus 5'UTR, including poliovirus, coxsackievirus, swine vesicular disease virus, echovirus, enterovirus, human rhinovirus, encephalomyocarditis virus, mengovirus, Theiler's murine encephalomyelitis virus, foot-and-mouth disease virus, hepatitis A and C viruses, bovine viral diarrhea virus, and hog cholera virus, indicates that the predicted conserved structural core is indeed a general structural feature for all members of the picornavirus, HCV and pestivirus families. Moreover, the common structural motif of these virus IRES share a similar structural feature to that determined in the structural core of the group I intron. The evolution of the common structural core likely occurred by the gradual substitution, addition or deletion of structural domains and elements to preserve a similar tertiary structure that facilitates the utilization of the IRES in specific host-cell environments.

M-AM-D4

AN RNA TOPOISOMERASE. ((Hui Wang, Russell J. Di Gate and Nadrian C. Seeman)) Department of Chemistry, New York University, New York, NY 10003 and Department of Pharmaceutical Science, University of Maryland, Baltimore, MD 21201.

A synthetic strand of RNA has been designed so that it can adopt two different topological states when ligated into a cyclic molecule, a circle and a trefoil knot. The RNA knot and circle have been characterized by their behavior in gel electrophoresis and sedimentation experiments. This system allows one to assay for the existence of an RNA topoisomerase, because the two RNA molecules can be interconverted only by a strand passage event. We find that the interconversion of these two species can be catalyzed by *E. coli* DNA topoisomerase III, indicating that this enzyme can act as an RNA topoisomerase. The conversion of circles to knots is accompanied by a small amount of RNA catenane generation. These findings suggest that strand passage must be considered a potential component of the folding and modification of RNA structures.

Supported by grants GM-29554 and GM-48445 from the NIH.

M-AM-D5

DETERMINATION OF CROSSOVER ISOMER DISTRIBUTIONS IN SYNTHETIC HOLLIDAY JUNCTIONS BY TIME-RESOLVED FRET. ((D. P. Millar and R. S. Fee)) Department of Molecular Biology, The Scripps Research Institute, La Jolla, CA 92037.

The Holliday junction (HJ) is a four-arm, four-strand branched DNA crossover structure formed during the course of genetic recombination. The three-dimensional structure of these DNA crossovers appears to be critical to their recognition and resolution into parental or recombined products. A consensus view of the HJ has emerged in which helical arms stack upon each other in a pairwise fashion forming two duplex domains with an acute interhelical angle. There are two possible arrangements (termed crossover isomers) for an HJ, depending on which arms stack with which. It is generally assumed that HJs exist in one predominant crossover isomer, according to the sequence of the four base pairs at the branching point, with the sequence of the rest of the molecule having no effect. On the basis of time-resolved measurements of fluorescence resonance energy transfer (FRET) between dyes attached pairwise to the junction arms, we demonstrate that HJs can exist as an equilibrium between both crossover isomers. Synthetic HJs were prepared with fluorescein (donor) and tetramethylrhodamine (acceptor) dyes attached to the 5' ends of particular duplex arms. The donor-acceptor distance was resolved into two Gaussian distributions, corresponding to the two crossover isomers, by analysis of the time-resolved emission profile of the donor dye following pulsed excitation. The isomer ratio was thereby determined for several 32 bp model HJs. The results confirm sequence-dependent variation in the extent of preference for one isomer over the other, and reveal a previously unrecognized dependence of HJ structure on the sequence adjacent to the branching point. Supported by NSF grant MCB-9317369.

M-AM-D6

STRUCTURE/FUNCTION RELATIONSHIP OF THE INSULIN-LINKED POLYMORPHIC REGION: IMPLICATIONS IN THE LENGTH POLYMORPHISM AND GENE REGULATION

Paolo Catasti[1,2], E. Morton Bradbury[2,3] and Goutam Gupta[1]
(1) Theoretical Biology and Biophysics, T-10, MS-K710. (2) Life Science Division, LS-2. MS-M880, Los Alamos National Laboratory, Los Alamos, NM 87501
(3) Department of Biological Chemistry, School of Medicine, University of California at Davis, Davis, CA 95616

The insulin-linked polymorphic region (ILPR), a 14 base-pairs-long tandem repeat 5'-ACAGGGGTGTGGGG-3' 3'-TGTCCCCACACCCC-5' is located 363 bases upstream of the human insulin gene. A locus for insulin-dependent diabetes mellitus (IDDM), an autoimmune disease, has been mapped to the ILPR. We show by 2D NMR analyses that both strands of the ILPR form multiply folded single-stranded structures. The G-rich strand of the ILPR adopts a telomere-like hairpin G-quartet structure with melting temperature of 85°C, whereas the C-rich strand forms intercalated hairpin structures with hemi-protonated parallel C≡C base pairs (i-motif) already at neutral pH, as proven by a combination of 1D NMR, CD, P1 digestion and gel electrophoresis. 1D NMR studies show that the ILPR forms hairpin structures even in presence of the complementary strand, with the equilibrium shifted toward the Watson-Crick duplex for neutral solutions (pH>6) and lower temperatures (T<37°C). Analyses of single and double mutations in the repeat sequence, reveal a direct correlation between the structure and stability of the ILPR hairpin structures. Interestingly, the same mutations that destabilize the hairpin structures also lower the transcriptional activity of the human insulin gene. We propose that the ILPR hairpin structures facilitate transcpription by creating negative supercoiling and single-strand specific hyper-sensitive sites behind RNA polymerase.

M-AM-D7

EFFECTS OF CHAIN LENGTH MODIFICATION AND BIS(ETHYL) SUBSTITUTION OF TETRA- AND PENTA- AMINE ANALOGS OF SPERMINE ON TRIPLEX DNA STABILIZATION, AGGREGATION AND CONFORMATIONAL TRANSITIONS. ((M. Musso, T. Thomas, A. Shirahata, L. H. Sigal, M. W. Van Dyke and **T.J. Thomas**)) UMDNJ-RWJ Med. Sch., New Brunswick, NJ 08903, Univ. Tex. M.D. Anderson Cancer Center, Houston, TX 77030, and Josai University, Saitama, Japan.

We studied the ability of 2 tetramine and 2 pentamine analogs of spermine, and their bis(ethyl) derivatives to stabilize triplex DNA formation between 5'-$TG_3TG_4TG_4TG_3T$-3' and its target duplex probe. We used electrophoretic mobility shift assay, Tm measurements, and CD spectroscopy to evaluate polyamine effects on triplex DNA stability, dissociation constants, aggregation, and conformation. In general, pentamines were more efficacious than tetramines in stabilizing triplex DNA, although most of the polyamines with pendant free amino groups caused DNA aggregation at <50% conversion to triplex DNA. Ethyl substitution of these pendant amino groups lowered their efficacy approximately 2-fold in stabilizing triplex DNA; however, this effect was more than compensated for by the lack of DNA aggregation. A concentration-dependent increase in the Tm was observed in the presence of polyamines. CD spectral measurements showed distinct differences in the conformation of triplex DNA in the presence of polyamines compared to the CD spectra of oligonucleotides. Temperature-dependent CD spectra of triplex DNA showed monophasic melting in the absence and presence of polyamines, suggesting duplex/triplex → single stranded DNA transition. These results indicate that structural modification of polyamines is an effective strategy to develop triplex DNA stabilizing ligands, with potential applications in anti-gene therapeutics.

PHOTOSYNTHESIS I

M-AM-E1

INTERACTION OF Q_B AND Q_B^- WITH THE PROTEIN IN NATIVE AND SER-L223→ALA *Rb. sphaeroides* REACTION CENTERS PROBED BY LIGHT-INDUCED FTIR DIFFERENCE SPECTROSCOPY

((J. Breton[1], E. Nabedryk[1], C Boullais[2], C. Mioskowski[2], M. L. Paddock[3], G. Feher[3], & M. Y. Okamura[3])) [1]SBE/DBCM, [2]SMM/DBCM, CEA-Saclay, Gif-sur-Yvette, France; [3]Department of Physics, UCSD, La Jolla, CA 92093

In *Rb. sphaeroides* reaction centers (RCs), the secondary quinone Q_B interacts with the protein forming hydrogen bonds. In particular, Ser-L223 has been proposed to hydrogen bond the C_1=O carbonyl of Q_B[1]. The technique of light-induced FTIR difference spectroscopy with specifically labeled quinones can help determine the strength of such interactions. In this study such measurements were made on native and Ser-L223→Ala mutant RCs[2] to investigate the interactions of Ser-L223 with Q_B and Q_B^-. The Q_B site was reconstituted with ubiquinone-3 (Q_3) selectively labeled with ^{13}C at the C_1 or the C_4 position. The molecular vibrations of Q_B can be specifically viewed by calculating a double-difference spectrum between the Q_B^-/Q_B spectra recorded with RCs reconstituted with ^{13}C-labeled and unlabeled Q_3, since protein contributions cancel. For native RCs, the double-difference spectra are distinctly different for $^{13}C_1$ and $^{13}C_4$ at the level of the C=C vibrations, although each carbonyl of Q_B is downshifted $\approx$10 cm^{-1} from solution values indicating equivalent but weak hydrogen bonding of the carbonyls to the protein[3]. The double-difference spectra for $^{13}C_1$ and $^{13}C_4$ in the Ser-L223→Ala mutant are essentially unchanged from those observed for native RCs. Thus, Ser-L223 does not have a strong interaction with either Q_B or Q_B^-. These conclusions are consistent with those obtained from ENDOR studies (see previous abstract by Paddock et al.).

[1]Allen *et al.*, 1988, *Proc. Natl. Acad. Sci. USA* 85, 8487. [2]Paddock *et al.*, 1990, *ibid.*, 87, 6602. [3]Breton *et al.*, 1995, *Biochemistry* 34, 11606.

M-AM-E2

A QUANTITATIVE TEST OF THE "LEAKY" Z-SCHEME OF PHOTOSYNTHESIS. ((**E. Greenbaum**[1], J. W. Lee[1], S. L. Blankinship[1], C. V. Tevault[1], and T. G. Owens[2])) [1]Oak Ridge National Laboratory, Oak Ridge, TN 37831, [2]Cornell University, Ithaca, NY 14853

It has recently been shown that *Chlamydomonas reinhardtii* mutants deficient in Photosystem (PS) I are capable of sustained simultaneous photoevolution of hydrogen and oxygen, photoassimilation of atmospheric CO_2 (1) and photoautotrophic growth (2). Using P700 absorption spectroscopy, an upper limit of 3-5% for the presence of functional PS I was determined. These data indicate that complete photosynthesis can be driven by the PS II light reaction alone. However, it has recently been postulated (3) that a low-level of undetectable PS I may be present in these mutants, i.e., the mutants are "leaky." According to this interpretation, a Z-scheme-like mechanism can be preserved by a rapid turnover of the PS I reaction centers, with a corresponding stoichiometric ratio of PS II to PS I of 20 or greater. The "leaky" Z-scheme model is capable of direct experimental test by measuring the absolute yields of hydrogen per single turnover saturating flash of light. In this presentation a comparative study of absolute hydrogen flash yields between wild-type and PS I-deficient mutants of *Chlamydomonas reinhardtii* will be presented.

(1) E. Greenbaum, et al., *Nature* **376**, 438 (1995); (2) J. W. Lee et al., *Science* **273**, 364 (1996); (3) V. A. Boichenko, *Photosyn. Res.* **47**, 291 (1996).

M-AM-E3

OBSERVATION OF THE PROTONATED SEMIQUINONE IN RCs OF Rb. SPHAEROIDES SUPPORTS THE TWO-STEP MECHANISM OF PROTON-ACTIVATED ELECTRON TRANSFER. ((**M.S. Graige**, M.L. Paddock, G. Feher & M.Y. Okamura)) Dept. of Physics, University of California San Diego, 9500 Gilman Dr., La Jolla, CA 92093.

A proton-activated electron transfer mechanism in which protonation of the semiquinone increases the driving force for the subsequent electron transfer step $[Q_A^-Q_B + H^+ \rightleftarrows Q_A^-(Q_BH) \rightarrow Q_A(Q_BH)^-]$ has been proposed for Q_B reduction in reaction centers (RCs) from *Rb. sphaeroides*.[1] A difficulty in confirming this mechanism is that electron and proton transfer steps are tightly coupled; only the initial and final states of the reaction are observed. Confirmation of this mechanism requires the observation of the protonated semiquinone state and quantitative correlation with the measured rate constant, $k_{AB}^{(2)}$. Since in RCs the protonated ubi-semiquinone intermediate is not observed, rhodoquinone (RQ) was substituted for native ubiquinone in the Q_B site to raise the pK_A of Q_BH and allow its observation. The optical absorption spectrum of rhodosemiquinone (fig. 1) changes with pH from that characteristic of a protonated semiquinone (pH 6) to that characteristic of an anionic semiquinone (pH 8.5),[2] with an observed pK of ~7.5. The observed rate constant (fig. 2) begins to decrease at the onset of the RQH titration as predicted by the two-step proton-activated electron transfer mechanism.[1] These results provide support for this mechanism in native bacterial RCs.

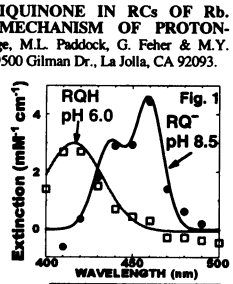

(1) Graige, M.S.; Paddock, M.L.; Bruce, J.M.; Feher, G.; Okamura, M.Y. **1996** *J. Am. Chem. Soc.* 118, 9005-9016. (2) Land, E.J.;Swallow, A.J. **1970** *J. Biol. Chem.* 226, 239-240. Supported by NIH and NSF. We thank J.M. Bruce for 2,3,6,7-tetramethyl-1,4-naphthoquinone which was used in the Q_A binding site.

M-AM-E4

MAPPING THE CYT c_2 BINDING SITE OF THE RC:CYT c_2 COMPLEX USING SITE-DIRECTED MUTAGENSIS ((**M. Tetreault**, S.H. Rongey, G. Feher, & M.Y. Okamura)) Dept. of Physics, UCSD, 9500 Gilman Dr., La Jolla, CA 92093-0319.

Cytochrome c_2 (cyt c_2) is a mobile electron carrier protein that serves as the secondary electron donor to the photosynthetic reaction center (RC) from *Rb. sphaeroides*. The ionic strength dependence of RC/cyt c_2 binding indicates that electrostatics are important for binding.[1] To identify residues on the periplasmic surface of the RC that govern the electrostatic attraction and binding of cyt c_2, surface Asp & Glu residues (see Fig.) were replaced with Lys. A dissociation constant, K_D (RC:cyt $c_2 \rightleftarrows$ RC + cyt c_2), for native and mutant RCs was obtained by measuring the fraction of cyt c_2 bound prior to a laser flash. Inter-protein electron transfer within the bound complex following light excitation is faster (τ ~ 1 μs) than the diffusion controlled second order rate (τ ~ 0.1 to 10 ms). The Glu-M184 → Lys replacement showed the largest change in cyt c_2 binding affinity with a K_D 600-fold larger than native.[2] The effects on binding of the other replacements decreased roughly with distance from the M184 site (see Fig.). The data suggest that the cyt c_2 binding site is located on the M subunit surface in the vicinity of M184, roughly consistent with models presented by Adir[3] and Tiede[4].

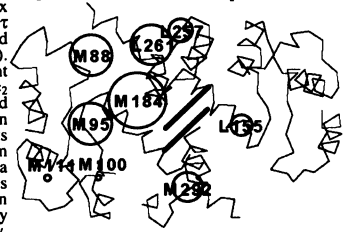

Periplasmic RC binding surface with carboxylic acid sites circled. Radii of circles are proportional to $\log(K_D)$; the largest circles indicate sites where the replacement with Lys had the largest effects on cyt c_2 binding. Dark lines indicate the position of the bacteriochlorophyll pair.

(1) Rosen *et. al.* **1980** *Biochem.* 19, 5687. (2) Adir *et al.* **1996** *Biochem.* 35, 8, 2535. (3) Tiede & Chang **1988** *Israel J. Chem.* 28, 183. Supported by NSF and NIH.

M-AM-E5

IDENTICATION OF HYDROGEN BONDS TO Q_B^- IN RCs OF *Rb. sphaeroides* BY ENDOR SPECTROSCOPY*

((M.L. Paddock, E. Abresch, R.A. Isaacson, G. Feher & M.Y. Okamura)) Phys. Dept., UCSD, La Jolla, CA 92093

The bacterial reaction center (RC) plays a central role in photosynthetic energy conversion by facilitating the double reduction and protonation of a bound quinone molecule, Q_B. ENDOR spectroscopy was used to investigate the hydrogen bonding of Q_B^- to nearby amino acid residues. Experiments were performed in native-like Zn^{2+}-RCs [1] and mutant Zn^{2+}-RCs in which Ser-L223 was replaced with Ala [2]. The ENDOR spectrum of native-like RCs shows two peaks, labeled "a" and "b" [3], that are strongly coupled to the unpaired electron on Q_B^- (see Fig.). Since the "a" and "b" peaks are present in the mutant RCs, neither the "a" or "b" peak can be due to the Ser-L223 hydroxyl proton as previously proposed [4]. Thus Ser-L223 is not hydrogen bonded (*i.e.* strongly coupled) to Q_B^-, consistent with recent FTIR results (see following abstract). Since the "a" peak is unaltered in the mutant RCs, it is assigned to an interaction between the O4 carbonyl oxygen of Q_B^- and His-L190. In contrast, since the "b" peak is split in the mutant RCs, part of the peak is assigned to an interaction between the O1 carbonyl oxygen of Q_B^- and the backbone NH of Ile-L224, located near Ser-L223 and within hydrogen bonding distance to Q_B^- (previous abstract). The other component of the "b" peak can be due to either a second hydrogen bond between O1 and the backbone (*e.g.* NH of Gly-L225) or to conformational heterogeneity. [1] These RCs contained a His-M266 → Cys mutation (Williams *et al.* (1991) *Biophys. J.*, **59**, 142a), which facilitates the replacement of Fe^{2+} by Zn^{2+}-RCs. [2] Paddock *et al.* (1990) *PNAS* **87**, 6602-6606. [3] Feher *et al.* (1985) *Springer Chem. Phys. Ser.* 42, p.174. [4] Paddock *et al.* (1995) *Biophys. J.* **68**, 246a.

*Supported by NSF & NIH

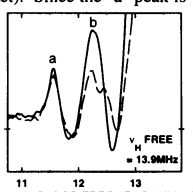

Low frequency Q_B^- ENDOR spectra (ν=9GHz, T=-30C) of NATIVE (solid) and Ser-L223 → Ala mutant (dashed) RCs.

M-AM-E6

A CRYSTALLOGRAPHIC INVESTIGATION OF LIGHT-INDUCED STRUCTURAL CHANGES IN REACTION CENTERS OF *Rb. sphaeroides*

((E.C.Abresch*, M.H.B. Stowell†, T.M. McPhillips†, D.C. Rees†, S.M. Soltis‡, and G. Feher*)) *Dept.of Physics, Univ.of Cal. San Diego, 9500 Gilman Dr., La Jolla, CA 92093-0319, †Calif. Inst. of Tech., Pasadena, CA 91125, ‡Stanford Synchrotron Research Lab., Stanford, CA

Structural changes accompanying charge separation $DQ_AQ_B \rightarrow D^+Q_AQ_B^-$ have been investigated in Reaction Centers (RCs) from *Rb. sphaeroides* R-26 by high resolution x-ray diffraction at ~90°K. Data sets were taken on RC crystals cooled in the dark and on crystals cooled under illumination to cryogenic temperatures. The structures were refined to 2.2Å and 2.6Å, respectively. In the light, charge separated state, the quinone has moved (see Q_B II in figure) from the position of the dark, charge neutral state (see Q_B I in figure) by ~5Å and undergone a 180° propeller twist around the isoprene chain. In the Q_B I position, the quinone O4 carbonyl H-bonds to the amide nitrogen of Ile-L224, and the O1 carbonyl forms no H-bond. In the Q_B II position, the quinone O1 carbonyl H-bonds to the amide nitrogen of Ile-L224, and the O4 carbonyl H-bonds to His-L190. We propose a model in which the movement of Q_B from its neutral position to its position in the charge separated state is a prerequisite for electron transfer from Q_A^- to Q_B. Work supported by the NIH.

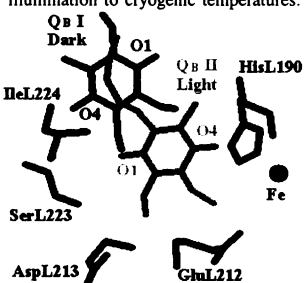

Superposition of quinone from dark and light structures and surrounding amino acid residues from dark structure

M-AM-E7

B-BRANCH ELECTRON TRANSFER IN BACTERIAL PHOTOSYNTHETIC REACTION CENTERS BY ENERGETICALLY ACTIVATING A-BRANCH CHARGE SEPARATION

((G. Hartwich, G. Bieser, T. Langenbacher, P. Müller, M. Richter, A. Ogrodnik, H. Scheer§, M.E. Michel-Beyerle))
Institut für Physikalische und Theoretische Chemie, TU München, Lichtenbergstr 4, 85748 Garching, Germany.
§ Botanisches Institut der Universität München, Menzingerstr 67, 80638 München, Germany

One of the fingerprint features of charge separation in the bacterial photosynthetic reaction center (RC) is its "exclusive" unidirectionality along one of two branches of cofactors (active A-branch, inactive B-branch) while x-ray data reveal almost no structural assymmetry on the cofactors. In order to increase the probability of B-branch electron transfer (ET), the initial ET step along the A-branch has been slowed down by increasing the energy of the state $P^+B_\lambda^-$ (B_λ is the monomeric bacteriochlorophyll (BChl) at the A-branch and is the first electron acceptor). This has been achieved by selectively exchanging the native Bchl at the site B_λ against Vinyl-BChl, which *in vitro* has a reduction potential ~150mV higher as compared to the native BChl. This modification results in an increase of the $^1P^*$ lifetime from 3 to 30ps at 290K and from 2 to 300ps at 90K. Above 180K an activation energy of 70meV is observed, below 180K the lifetimes become temperature independent, reflecting the freezing of $P^+B_\lambda^-$ formation and the takeover of temperature independent formation of the next acceptor state $P^+H_\lambda^-$ via the superexchange mechanism.

Aside from the transient bleaching of the H_λ-absorption at 546nm, an additional bleaching of H_H at 533nm remains evident after correcting for electrochromic shifts induced by P^+, indicating ET along the unmodified B-branch. The bleaching of H_H vanishes in case B_H is also exchanged against Vinyl-BChl. The ns-lifetime of the H_H signal is independent of the presence of (i) Q_A, corroborating the assignment to H_B and of (ii) Q_H, indicating that ET to Q_H cannot compete with recombination of $P^+H_H^-$. This can be understood in terms of different reorganisation energies for the transfer of an electron to Q_λ and Q_H due to the nature of the binding site of the fixed and of the shuttle quinone. We rate this incapability of efficient ET from H_H to Q_H as the functional necessity for unidirectionality. From the quantum yield of $P^+H_H^-$ formation, the rate of charge separation along the B-branch at 90K is estimated to be $(2\text{-}3ns)^{-1}$, implying an A/B branching ratio of charge separation in native RCs of 1000/1. The physical origin for unidirectionality predominantly resting on energetic differences of the involved radical pair states rather than on different electronic couplings is concluded from the similarity of $P^+H_\lambda^-$ and of $P^+H_H^-$ recombination dynamics.

MOLECULAR APPROACHES TO TRANSMEMBRANE SIGNALING

M-AM-SymII-1 **J. Falke, University of Colorado**
Molecular Mechanism of Transmembrane Signaling by the Aspartate Receptor

M-AM-SymII-2 **D. Trentham, National Institute for Medical Research, England**
Mechanisms of Chemotactic Signaling Probed by Caged Ligands

M-AM-SymII-3 **L. J. Kenney, Oregon Health Sciences University**
The Role of Phosphorylation in Osmoregulatory Signaling by OmpR

M-AM-SymII-4 **J. Spudich, University of Texas Medical School**
Signaling by an *Archaeal* Seven-helix Photosensory Receptor

M-AM-F1

SOLUBILIZING EFFECT OF NITRIC OXIDE ON DEOXYHEMOGLOBIN S SOLUTIONS AND SICKLE HEMOLYSATES. ((**W.A. McDade**, H.M. Shaba, and N. Carter)) University of Chicago, Department of Anesthesia and Critical Care, Chicago, IL 60637.

Patients in sickle crisis may derive benefit from inhaled NO to improve vasoconstriction and vasoocclusion. However, there are potential biochemical hazards in exposing patients with sickle cell disease to NO. Polymerization of HbS only occurs in the deoxygenated state. Should nitrosyl sickle hemoglobin assume of a configuration more T- than R-state in nature, its globin chains may assume a more deoxy-like state, capable of polymerization. Briehl and Salhany (1975) observed the gelation properties of nitrosyl sickle hemoglobin and concluded that inositol hexaphosphate treated nitrosyl sickle hemoglobin is in a T-state configuration. These findings support the hypothesis that sickle nitrosylhemoglobin may polymerize. We now present work assessing the ability of NO to alter the solubility of sickle hemoglobin solutions. In saturated NO, purified deoxyHbS does not polymerize. We present data on the effect of decreasing concentrations of NO on deoxyHbS saturation concentration. To ascertain the ability of intracellular polymerization, hemolysates of deoxygenated sickle erythrocytes were exposed to NO in varying concentrations and the hemoglobin solubility determined by ultracentrifugation. Our current data suggest that NO does not cause increased HbS polymerization in purified solutions or dilute hemolysates.

References:
Briehl RW, Salhany JM. Gelation of sickle hemoglobin. III. Nitrosyl hemoglobin. Journal of Molecular Biology 96: 733-43,1975.

M-AM-F2

MEASUREMENTS OF FREE AND ENCAPSULATED HEMOGLOBIN OXIDATION BY EPR SPECTROSCOPY. (([a]**O.O. Abugo**, [a]V.W. Macdonald, [‡]A.S. Rudolph,[a]J.R. Hess, [f]C. Balagopalakrishna, and [f]J.M. Rifkind)) [a]Blood Research Detachment, Walter Reed Army Institute of Research, Washington, DC; ‡Center for Bio/Molecular Science and Engineering, Naval Research Laboratory, Washington, DC; and [f]Gerontology Research Center, National Institute on Aging, National Institutes of Health, Baltimore, MD. (Spon. by R.L. Berger)

Direct measurements of the autoxidation of liposome encapsulated hemoglobin (LEH) are difficult to carry out using conventional UV-Visible spectroscopy because of the high turbidity of the LEH samples. Electron paramagnetic resonance (EPR) spectroscopy is not affected by sample turbidity. Higher protein concentrations simply enhance the EPR spectroscopic signal. In this study, samples of free and liposome encapsulated human hemoglobin cross-linked between alpha chains with bis (3,5-dibromosalicyl) fumarate ($\alpha\alpha$Hb) in Ringers Acetate were introduced into EPR tubes and incubated at 37°C for 1 to 80 hours. Oxidation reactions of sample pairs were quenched at specific time intervals by submersion of EPR tubes in liquid nitrogen. Extended incubation for 168 hours of one sample pair was performed in order to obtain EPR spectra of fully oxidized hemoglobin. The amount of oxidized hemoglobin was determined by measuring EPR spectra at 7°K using an IBM ER-200D-SRC spectrometer with 100-KHz modulation. Acquired spectra included the dominant high spin tetragonal complex with $g_\perp$=6.0 and $g_\parallel$=2.0, and the minor low spin complexes (hemichromes) with g values ranging from 1.63 to 2.98. Rate constants for the oxidation were determined by the exponential curve fit of the variation of formed metHb with time. MetHb levels were determined by the double integration of the EPR first derivative spectra between the regions of 1000 to 3800 gauss. Rate constants of 0.0425 hr^{-1} and 0.0693 hr^{-1} for the $\alpha\alpha$Hb and LEH samples respectively implied that the oxidation of the $\alpha\alpha$Hb was only slightly enhanced by the liposome encapsulation. The results obtained also showed a shift in the g value and substantial enhancement of the intensity of the water containing bis-histidine low spin complex for the encapsulated hemoglobin.

M-AM-F3

THE CONFORMATION OF THE HEME IS CONSERVED IN PROTEINS OF THE SAME FUNCTIONAL CLASS. ((**W. Jentzen**,[1] J. A. Shelnutt[1,2])) [1]Fuel Science Department, Sandia National Laboratories, Albuquerque, NM 87185-0710. [2]Department of Chemistry, University of New Mexico, Albuquerque, NM 87131.

The out-of-plane distortions of heme groups from proteins have been characterized in terms of equivalent displacements along the lowest-frequency out-of-plane normal coordinates of the D_{4h}-symmetric porphyrin macrocycle. The X-ray crystal structures retrieved from the Protein Data Bank were analyzed using a computational procedure for determining these displacements. The X-ray crystal structures of the heme groups are described adequately by using only the lowest-frequency normal coordinate of each symmetry type. That is, a linear combination of the normal deformations of the saddling (*sad*, B_{2u}), ruffling (*ruf*, B_{1u}), doming (*dom*, A_{2u}), waving [*wav*(*x*), *wav*(*y*); E_g], and propellering (*pro*, A_{1u}) symmetry types accurately simulates the out-of-plane distortion of the heme groups in proteins. For example, the structural decomposition of the heme groups in deoxymyoglobin shows that each of the hemes exhibits a predominantly *dom* deformation with a smaller but significant *wav*(*y*) deformation. Furthermore, examination of the decomposition results for the X-ray crystal structures of different types of cytochromes reveals that in many cases the heme conformation is found to be conserved for different species and also characteristic of each functional class. Moreover, the covalently linked heme groups in cytochromes c_3 and mitochondrial cytochromes *c* from different species show a large variation in their amino acid sequence, yet the heme groups in each species exhibit similar heme conformations as long as the short peptide sequences between the cysteine linkages are homologous. However, differences in heme conformations are noted when the amino acid sequence of this short fragment varies in number and types of residues. This suggest that this small covalently linked protein segment plays a central role in the nonplanar heme conformation in *c*-type cytochromes. [Supported by United States Department of Energy Contract DE-AC04-94DP85000 (J.A.S.) and a postdoctoral fellowship (W.J.).]

M-AM-F4

BIOPHYSICAL AND BIOCHEMICAL STUDIES OF RECOMBINANT MUTANT HEMOGLOBINS WITH LOW OXYGEN AFFINITY ((**Dazhen Philip Sun**, Chih-Kao Hu, Zhen-Yu Sun, Tong Jian Shen, Nancy T. Ho, and Chien Ho, Department of Biological Sciences, Carnegie Mellon University, Pittsburgh, PA 15213))

We have investigated a number of recombinant mutant hemoglobins (r Hbs) with low oxygen affinity using the techniques of equilibrium oxygen binding, stopped-flow kinetics, and ^{1}H nuclear magnetic resonance (NMR) spectroscopy. These r Hbs have mutations in the $\alpha_1\beta_2$ subunit interface and exhibit low oxygen affinity compared to that of human normal adult hemoglobin (Hb A). ^{1}H-NMR results of r Hb (α96Val→Trp), r Hb Presbyterian (β108Asn→Lys), and r Hb (α96Val→Trp, β108Asn→Lys) indicate that these three r Hbs can be switched to the deoxy (T) quaternary conformation, even when the hemes in these r Hbs are bound to CO. Stopped-flow experiments are being carried out to investigate the kinetics of ligand binding of these three r Hbs. Results from our experiments suggest that the extra stability of the deoxy quaternary structure is the likely reason which gives rise to the low oxygen affinity of these three r Hbs. These results have implications for designing hemoglobins suitable for hemoglobin-based oxygen carriers. [Supported by research grants from NIH].

M-AM-F5

CONFORMATIONAL HOMOGENEITY OF NICKEL(II) *MESO*-TETRAPHENYLPORPHYRIN TRIGGERED BY AXIAL LIGATION AND NEW EVIDENCE FOR EXISTENCE OF THE 5-COORDINATED SPECIES ((**S.-L Jia**,[1,2] X.-Z. Song,[1,2] W. Jentzen,[1] J.-G. Ma,[1,2] and J. A. Shelnutt[1,2])) [1] Fuel Science Department, Sandia National Laboratories, Albuquerque, NM 87185-0710. [2] Department of Chemistry, University of New Mexico, Albuquerque, NM 87131.

The axial ligation of nickel(II) *meso*-tetraphenylporphyrin (NiTPP) in pyrrolidine is investigated with molecular mechanics (MM) calculations, UV-visible absorption spectroscopy and resonance Raman (RR) spectroscopy. The clear evidence for 5-coordinated species (Ni(Pyr)TPP) was found with RR spectroscopy. Like the 6-coordinated species ($Ni(Pyr)_2TPP$), the formation of Ni(Pyr)TPP can be monitored with the oxidation-state marker line ν_4, by varying the concentration of pyrrolidine in a non-coordinating solvent (dicloromethane). At low concentration of pyrrolidine, two new ν_4 lines appear, down-shifted by 26 and 19 cm^{-1}, respectively, from the ν_4 line of NiTPP. These two new lines are for $Ni(Pyr)_2TPP$ and Ni(Pyr)TPP, respectively. Also, this region is complicated by another line (ν_{29}) which appears between the ν_4 lines of NiTPP and Ni(Pyr)TPP. At high concentration of pyrrolidine, the 6-coordinated species dominates and ν_4 line for Ni(Pyr)TPP is obscured by ν_4 for $Ni(Pyr)_2TPP$. Line shifts are also observed for the structure sensitive lines ν_2 and ν_8 lines upon axial ligation of NiTPP. Further, broad, asymmetric ν_2 and ν_8 for NiTPP indicate the coexistence of different conformers. Upon axial ligation, these two lines become sharp and symmetric, implying only one conformer. MM calculations indicate that there are three stable conformers for NiTPP. These are ruffled, saddled, and planar forms. However, there is only one nearly planar conformer for Ni(Pyr)TPP or $Ni(Pyr)_2TPP$. Structural parameters for both axially ligated porphyrins are almost same; thus, no shifted lines are observed for ν_2 and ν_8 for Ni(Pyr)TPP and $Ni(Pyr)_2TPP$ and the lines are narrow. (Supported by United States Department of Energy Under Contract DE-AC04-94AL85000).

M-AM-F6

METAL-DEPENDENCE OF THE RELATIVE CONTRIBUTIONS OF THE LOWEST-FREQUENCY NORMAL COORDINATES TO THE STERICALLY-INDUCED DISTORTIONS OF 5,15-DI-SUBSTITUTED PORPHYRINS ((**X.-Z. Song**,[1,2] W. Jentzen,[1] S.-L. Jia,[1,2] J.-G. Ma,[1,2] L. A. Jaquinod,[3] D. J. Nurco,[3] G. J. Medforth,[3] K. M. Smith [3] and J. A. Shelnutt[1,2])) [1]Fuel Science Department, Sandia National Laboratories, Albuquerque, NM 87185-0710. [2]Department of Chemistry, University of New Mexico, Albuquerque, NM 87131. [3]Department of Chemistry, University of California, Davis, CA 95616.

The influence of the central metal on the structure of the macrocycle for a series of 5,15-di-substituted metalloporphyrins has been investigated with X-ray crystallography, molecular mechanics (MM) calculations, UV-visible absorption and resonance Raman spectroscopy. MM calculations show that the series of porphyrins are predominantly in a gabled (*gab*) conformation consisting of a linear combination of *ruf* (B_{1u}) and *dom* (A_{2u}) normal deformation types. The calculated *gab* structures were structurally decomposed into equivalent displacements along the lowest-frequency normal coordinates of these symmetry types. The contributions of each of the normal coordinate to the total distortion agrees well with the contributions obtained by structurally decomposing the X-ray crystal structures. Changing the size of the central metal causes a change in the ratio of *dom*/*ruf* contributions. A large metal like zinc disfavors ruffling over doming, significantly reducing the ruffling contribution and slightly increasing the doming contribution. In addition, the total degree of nonplanar distortion is reduced. This is confirmed by the smaller red-shifts of the absorption bands and smaller down-shifts of the structure-sensitive Raman lines for the larger metals in the series of metalloporphyrins. (Supported by United States Department of Energy Contract DE-AC04-94AL85000.)

M-AM-F7

PHYSICOCHEMICAL CHARACTERISTICS AND POSSIBLE BIOLOGICAL ROLES OF THE [2Fe-2S] CLUSTER IN MAMMALIAN FERROCHELATASE. ((**R. Franco** [1,2], S.G. Lloyd [3], J.J.G. Moura [2], I. Moura [2], B.H. Huynh [3] and G.C. Ferreira [1]) [1] Dept. of Biochem. and Mole. Biol., Coll. of Medicine, Univ. of South Florida, Tampa, FL 33612, [2] Dept. de Química and Centro de Química Fina e Biotecnologia, Univ. Nova de Lisboa, 2825 Monte de Caparica, Portugal, [3] Dept. of Physics, Emory Univ., Atlanta, GA 30322 (Spon. by G.C. Ferreira)

The recently discovered [2Fe-2S] cluster in mouse liver ferrochelatase has been characterized using UV-Visible, EPR, and Mössbauer spectroscopic techniques. Studies are reported here for the recombinant protein purified from an overproducing transformed *E. coli* strain. The as-isolated ferrochelatase [2Fe-2S] cluster exhibits a UV/Vis absorption band centered at 330 nm with distinct shoulders at 440 and 525 nm, indicative of a $[2Fe\text{-}2S]^{2+}$ cluster, and is EPR-silent, suggesting a diamagnetic ground state. This is confirmed by the 8 T Mössbauer spectrum of the ^{57}Fe-enriched as-isolated protein, which is well simulated by parameters ΔEQ =0.69±0.03 mm/s and δ=0.28±0.02 mm/s and assuming diamagnetism. Upon reduction with sodium dithionite, ferrochelatase shows a near-axial EPR spectrum with g-values of 2.00, 1.93, and 1.91, consistent with a Fe(III) site antiferromagnetically coupled with a Fe(II) site to yield a S=1/2 ground state. Redox titrations monitored by UV-Visible and EPR spectroscopy reveal midpoint potentials of –390 ± 10 mV and –405±10 mV, respectively. Mössbauer spectra of the sodium dithionite-reduced ^{57}Fe-enriched ferrochelatase continued to show magnetic hyperfine interactions at temperatures up to 220 K. Spectra collected at 4.2 K in the presence of magnetic fields of 60 mT and 8 T strengths were analyzed in the mixed-valent S=1/2 ground state. Certain differences from other well characterized [2Fe-2S]$^{+}$ cluster-containing proteins exist and are discussed. For the recombinant ferrochelatase, a positive correlation is observed between the presence of the [2Fe-2S] cluster and the enzymatic specific activity. Possible biological functions for the cluster are discussed. These include a redox role, a structural role, a regulatory role, or a combination of some of these four possibilities.

M-AM-F8

THE NONPLANARITY OF THE HEME IN CYTOCHROMES *C* IS ASSOCIATED WITH THE PEPTIDE SEGMENT BETWEEN THE CYSTEINE LINKAGES ((**J.-G. Ma,**[1,2] W. Jentzen,[1] M. Laberge,[3] J. Vanderkooi,[3] X.-Z. Song,[1,2] S.-L. Jia,[1,2] J. D. Hobbs,[1] J. A. Shelnutt[1,2])) [1]Fuel Science Department, Sandia National Laboratories, Albuquerque, NM 87185-0710. [2]Department of Chemistry, University of New Mexico, Albuquerque, NM 87131. [3]Department of Biochemistry and Biophysics, University of Pennsylvania, Philadelphia, PA 19104-6089.

Molecular mechanics (MM) calculations, UV-visible absorption and resonance Raman spectroscopy have been used to investigate nickel(II)-reconstituted cytochrome *c*, nickel(II) MP-11(micro-peroxidase), and some model nickel(II) porphyrins that simulate the effect of protein environment on the heme conformation in cytochromes *c*. MM calculations on mitochondrial cytochromes *c* support the proposal that the heme distortion is mainly induced by a relatively small protein segment consisting of the two covalently linked cysteines, the amino acids between two cysteines, and the axial-ligated histidine. Resonance Raman and UV-visible absorption spectra of nickel(II) cytochrome *c* show that the ligation state of nickel(II) cytochrome *c* is pH dependent. Axial ligands are present near neutral pH, but dissociated at the pH extremes. Upon raising the pH from 3.2 to 3.6, nickel picks up at least one axial ligand. At pH values for which nickel(II) cytochrome *c* is four-coordinate, both planar and nonplanar conformers coexist in solution. The amount of the nonplanar conformer increases relative to the planar conformer upon raising the pH from 1.0 to 3.0. The variation in the relative amount of these two conformers is probably a result of formation of the hydrogen bonding network in the peptide backbone as the pH is raised. This conclusion is supported by MM calculations on nickel(II) and heme penta-peptide, that is, the total degree of nonplanar distortion of the macrocycle increases when the hydrogen bonding is turned on in the calculation. Studies on nickel(II) MP-11 also show that the peptide backbone exerts a force on the macrocycle distortion. (Supported by the U.S. Department of Energy under contract DE-AC04-94AL85000).

M-AM-F9

IDENTIFICATION OF PUTATIVE PEROXIDE INTERMEDIATES OF PEROXIDASES BY ELECTRONIC STRUCTURE AND SPECTRA CALCULATIONS

((**G.H. Loew** and D.L. Harris)) Molecular Research Institute, Palo Alto, California 94304

In the enzymatic cycle of this family of oxidative metabolizing heme proteins, hydrogen peroxide is required to transform the ferric resting state to the catalyltically active, ferryl Fe=O, Compound I species. While a peroxide complex has been proposed as a key intermediate in this reaction, this species is is too transient to have thus far been definitively characterized, Electronic spectra observed prior to compound I formation during the reaction of H_2O_2 with both wild type and R38L HRP-C have been attrubuted to this intermediate. There are however significant qualitative differences in these spectra in the 300-450 nm region, with an extra hyper-Soret band observed in one and a normal Soret, not very different from the resting state found in the other. In the absence of any additional information, it is not possible from these spectra alone to identify the species that gives rise to them or to understand these differences. To further identify the origin of these spectra and their differences, the INDO/RHF/CI quantum chemical method has been used to calculate the electronic structure and spectra of two candidate peroxide intermediates of model peroxidases, one with a neutral peroxide and the other with an anionic form(OOH-) as the heme Fe ligand. Comparision of the calculated spectra with the observed spectra, led to the identification of the transient species responsible for each of these spectra and could account for the observed differences between them. The "hyper-porphyrin " spectrum obsrved in the wtHRP-C experiments was found to originate from the OOH- form of this transient intermediate in a low spin ground state, while the normal Soret observed in the R38Lmutant experiment originated from the neutral peroxide form in a high spin ground state. These results allow for the first time a one to one correspondence to be made between the observed spectra and the species that could be causing them, and provide further evidence for transient peroxide intermediates in the pathway from the resting state to Compound I of peroxidases.

K CHANNELS: ASSEMBLY/LOCALIZATION

M-AM-G1

STEPS IN THE ASSEMBLY OF SHAKER K^+ CHANNELS PROBED BY MUTATIONS IN TRANSMEMBRANE SEGMENTS. ((**C.T. Schulteis,** N. Nagaya, and D.M. Papazian)) IDP Neuroscience and Physiology Dept., UCLA School of Medicine, Los Angeles, CA 90095.

The biogenesis of voltage-gated K^+ channels involves the folding of individual subunits and the assembly of pore-forming α and cytoplasmic β subunits. To characterize the interplay of folding and assembly steps during the biogenesis of Shaker channels, we have determined the effect of two mutations that disrupt subunit folding, D316K in S3 and K374E in S4, on the formation of three previously-identified quaternary interactions: 1) a homotypic interaction between the N-termini of Shaker α subunits that is critical for their assembly, 2) an interaction between α and β subunits mediated by the N-terminus of the α subunit, and 3) an interaction between N- and C-termini of adjacent α subunits detected in native channels by the oxidation of a disulfide bond between C96 and C505. Both D316K and K374E exert a dominant negative effect on the expression of Shaker-IR in *Xenopus* oocytes. This effect is mediated by amino acids 96-197 in the N-terminal, as deletion of this domain eliminates the dominant negative effect. Therefore, these folding mutations do not prevent the establishment of the homotypic interaction critical for α subunit assembly. In addition, the folding mutations do not prevent the co-assembly of α and β subunits, as demonstrated by co-immunoprecipitation in transfected cells. However, the folding mutations do disrupt the establishment of the proximity between the N- and C-termini of adjacent α subunits, because intersubunit disulfide bonds fail to form between C96 and C505 in mutant subunits. The double mutation, D316K+K347E, which rescues the folding defects of the individual mutants, restores the C96/C505 interaction. Our results suggest that assembly steps mediated by the N-terminus occur independently of folding of the transmembrane segments. However, proper folding of transmembrane segments is required to establish the proximity between the N- and C-termini of adjacent α subunits, which is characteristic of native channels. Supported by the NIH, the Keck Foundation, HHMI (CTS), and AHA-GLAA (NN).

M-AM-G2

MOLECULAR DETERMINANTS OF KIR3.0 CHANNEL ASSEMBLY

((**R. Woodward,** E.B. Stevens and R.D. Murrell-Lagnado)) Dept. of Pharmacology, University of Cambridge, Tennis Court Rd, Cambridge CB2 1QJ, UK.

Members of the Kir3 subfamily of cloned K^+ channel subunits form G-protein activated, inwardly rectifying K^+ channels. Kir3.1 forms functional heteromeric complexes with both Kir3.4 and Kir3.2 but does not form homomeric complexes. We have used *in-vitro* translation and co-immunoprecipitation analysis to investigate the molecular determinants involved in Kir3 subunit co-assembly. Truncated Kir3.1 constructs that encode either the core-region, the N-terminal region or the C-terminal region were all co-precipitated with both the full length Kir3.1 and Kir3.2 subunits. This suggests that regions involved in inter-subunit recognition are distributed throughout the Kir3 polypeptides. Non-overlapping C- and N-terminal polypeptides did not co-immunoprecipitate, suggesting that within a channel complex N-terminal domains interact with neighbouring N-terminal domains and C-terminal domains with neighbouring C-terminal domains. The interaction between the Kir3.1 C-terminal region and full-length Kir3.1 was of much higher affinity than between this region and Kir3.2, whereas the core- and N-terminal regions interacted with similar affinity with both Kir3's. We tested the ability of truncated Kir3.1 constructs to co-precipitate with Kir2.1 and found that the core-region was recognized by Kir2.1 whereas the C-terminal domain of Kir3.1 was not. These results suggest that the C-terminal region of Kir3.1 plays a discriminatory role in the process of channel assembly. Competition experiments in *Xenopus* oocytes in which Kir3.1 and Kir3.2 cRNAs were co-injected either with or without truncated Kir3.1 cRNAs showed that the body construct alone reduced Kir3.1/3.2 channel expression but constructs encoding the core-region plus increasing lengths of the hydrophilic regions competed with increasing effectiveness. Chimeric subunits were constructed in which the N- and C-terminal domains of Kir3.1 were substituted for those of Kir3.2, either individually or together. The ability of Kir3.1 to form heteromeric channels with any of the three chimeric subunits was dramatically reduced when compared with wild-type Kir3.1/3.2 expression levels. This provides further evidence for the involvement of Kir3 cytoplasmic domains in the channel assembly process.

M-AM-G3

RNA EDITING OF SQUID Kv2 K^+ CHANNELS: THE EFFECT OF CHRONIC TEMPERATURE CHANGE. ((**D.E. Patton** and F. Bezanilla))
UCLA, Departments of Physiology and Anesthesiology, Los Angeles, CA 90095.

We have previously reported that RNA editing generates functionally diverse sqKv2 K+ channels in the squid optic lobe (Patton and Bezanilla, *Biophys. J.* A13, 1996). To explore the possibility that this process is regulated by temperature, *Loliguncula brevis* were maintained at either 14°C or 24°C. The animals in the 14°C group exhibited severe behavioral abnormalities when initially exposed to the cooler temperature, but their behavior returned to normal within 24 hours. After 10 days at 14°C or 24°C, the mRNA isolated from the optic lobes of individual animals was subjected to RT-PCR using primers specific for sqKv2. PCR products were cloned and recombinants were sequenced between S4 and S6. The cDNA sequences were compared to genomic sequences derived by PCR from the same animal. Guanosines in the cDNA's were considered to be edited if the same position was occupied by an adenosine in the genomic DNA. To date, a total of 42 cDNA sequences from 2 animals in the 14°C group and 51 cDNA sequences from 2 animals in the 24°C group have been analyzed. One editing site, which changes a serine codon to a glycine codon in S6, was edited at an average efficiency of 31% (range: 25%-33%) in the 14°C group and 51% (range: 50%-52%) in the 24°C group. The editing efficiency at 2 highly edited sites near the S/G site was not affected by temperature. There is also a rare edit that converts a glutamine codon to an arginine codon in the S4 at a position equivalent to R362 in *Shaker*. All of the other Kv2 channels cloned so far have a glutamine in this position. This site was edited an average of 2% in the 14°C group and 6% in the 24°C group. These results indicate that RNA editing may be regulated by temperature in a site specific manner. Supported by NIH grants GM 30376 and RR01024.

M-AM-G4

EXPRESSION OF SPLIT SHAKER K CHANNELS IN XENOPUS OOCYTES. ((**D. Naranjo**, L. Kolmakova-Partensky and C. Miller)) HHMI, Department of Biochemistry. Brandeis University, Waltham MA 02254

In *Drosophila*, the family of Shaker K channels results from alternatively spliced products of the *Shaker* locus. A conserved central region is flanked by variables 5' and 3' ends leads to a diversity of K channel proteins. Do exons represent different structural domains of the protein?. We engineered a few Shaker B channel sequences with split points near the 3' border of the conserved central region (S3-S4 loop). We constructed N-terminal fragments with and without the 6-46 deletion responsible for the N-type inactivation kinetics. We also made C-terminal fragments carrying mutations in the vestibule loop that confer specific sensitivities to α-K-toxins. The cRNAs from these fragments were co-injected in *Xenopus* oocytes and channel expression examined with the two-electrode voltage-clamp technique. The expressed currents resembled the kinetics and selectivity of the wild-type channel. Voltage-dependent activation is displaced ~+20 mV. Inactivation kinetics and toxin sensitivity were as expected from the N- and C-terminal fragments used. These results are consistent with the notion that these two different regions in the channel sequence code for separate structural domains. Partially supported by GM-31768.

M-AM-G5

INTERSUBUNIT INTERACTION IN OPEN CNG CHANNELS. ((S.E. Gordon and W.N. Zagotta)) University of Washington, HHMI, Box 357370, Seattle, WA 98195-7370.

The photoreceptor cyclic nucleotide-gated (CNG) channels transduce photon absorption into changes in membrane potential and [Ca2+]i. Although they are activated by the direct binding of cGMP (and, to a much lesser extent, cAMP), CNG channels are structurally related to the voltage-gated family of ion channels. In this study, we investigated the architecture of the channel using copper/phenanthroline (CP), a reagent that promotes the formation of disulfide bonds between cysteine residues. Formation of such a disulfide bond is an indication of proximity between two cysteine residues. Using excised patches from oocytes expressing subunit 1 of the bovine rod CNG channel, we found that exposure to CP shifted the dose-response curve for activation by cGMP toward lower [cGMP], while decreasing its slope, and increased the maximal current activated by cAMP. These effects were observed only when CP was applied in combination with cGMP, indicating that cross-linking could occur only when the channels were activated. The potentiation was absent in channels which contained a mutation of either a cysteine in the amino terminal domain (C35) or a cysteine in the carboxy terminal domain (C481). Experiments in which subunits containing a mutation at C35 were coexpressed with subunits containing a mutation at C481 indicate that the disulfide bond was formed between residues of different subunits. Finally, detection of disulfide bond formation in channels formed from both subunit 1 and subunit 2 demonstrate that this type of interaction can occur in channels more closely resembling those in native photoreceptors.

M-AM-G6

LOCALIZATION OF HETEROLOGOUSLY EXPRESSED G-PROTEIN-GATED K^+ CHANNEL SUBUNITS. ((D. E. Logothetis, K. W. Chan, M. Yoshida and M. Sassaroli)) Departments of Physiology and Biophysics and Molecular Biology, Mount Sinai School of Medicine, CUNY, New York, NY 10029.

G-protein-gated inwardly rectifying K^+ (GIRK) channels appear to function as heteromultimers. Five related clones have been identified thus far (GIRK2-GIRK5). GIRK1 is unique in the GIRK channel subfamily in that although it is by itself inactive, it can associate with other family members to produce functional channels. Green fluorescent proteins (GFPs) have been used successfully as fusion tags to monitor protein localization within living cells. We have fused recombinant GFP to the carboxy terminal end of GIRK1 and GIRK4 subunits, and expressed them in *Xenopus* oocytes and mammalian CHO-K1 cells. GFP-tagged GIRK subunits showed functional characteristics indistinguishable from those of their non-tagged equivalents. Using confocal microscopy, channel subunits were localized by the fluorescence signal of the associated GFP tag. GIRK1-GFP showed mainly cytoplasmic localization, while GIRK4-GFP showed strong localization in the plasma membrane. Coexpression of GIRK1-GFP with non-tagged GIRK4 showed transfer of the fluorescence signal to the plasma membrane. This result suggests that the failure of GIRK1 to express significant homomeric channel currents may be due to its inability to be targeted to the plasma membrane, a task accomplished by its association with GIRK4. Total crude membranes isolated from oocytes expressing GIRK1-GFP or GIRK4-GFP were solubilized and when excited at 470 nm gave the expected fluorescence spectra of GFP. Quantification of protein level by fluorescence may provide us with estimates of the cytoplasmic versus plasma membrane pools of GIRK channel subunits.

M-AM-G7

PROBING THE INTERACTIONS WITH G-PROTEINS OF GIRK1 AND GIRK4, THE TWO SUBUNITS OF THE K-ACh CHANNEL, USING FUNCTIONAL HOMOMERIC MUTANTS

((**M. Vivaudou**, K.W. Chan, J.L. Sui & D.E. Logothetis)) Dept of Physiology & Biophysics, Mount Sinai School of Medicine, New York, NY 10029

In heart and brain, G-protein activated channels are complexes of 2 homologous proteins, GIRK1 and either GIRK4 or GIRK2.

The residue F137, located within the presumed pore region of GIRK1, plays a critical role in controlling the activity of GIRK1 homomers and GIRK1/GIRK4 heteromers (Chan et al, Proc Natl Acad Sci, in press). By modifying this residue, or the matching residue of GIRK4, S143, we have been able to produce mutant proteins which produced large inward-rectifying, G-protein-modulated, currents when expressed alone in Xenopus oocytes.

The availability of such mutants, which presumably form homomeric channels, allows the study of the individual properties of the subunits of heteromeric G-protein gated channels, and therefore of the contribution of each constituent subunit to the properties of the assembled channel.

In this work, we have investigated the receptor- and G-protein-mediated modulation of each of two active mutants, GIRK1(F137S) and GIRK4(S143T). These mutant subunits responded in a very similar manner to a number of tests involving coexpression with muscarinic receptors, G-protein native and mutated α subunits, G-protein βγ subunits, and pertussis toxin treatment. Therefore, GIRK1(F137S) and GIRK4(S143T), and by extrapolation their wild-type counterparts, interact in a qualitatively similar way with G-protein subunits. This finding suggests that the sites of interaction with G-protein subunits are located within the homologous regions of GIRK1 and GIRK4, and not within the divergent regions like the N and C terminal regions.

M-AM-G8

PHYSICAL ASSOCIATION OF A SULFONYLUREA RECEPTOR, SUR1, WITH INWARD RECTIFIER, $K_{IR}6.x$, SUBUNITS. ((**J.P. Clement IV**[1], G. Gonzalez[1], M. Schwanstecher[3], U. Panten[3], L. Aguilar-Bryan[2] and J. Bryan[1])), Depts. Cell Biology[1] and Medicine[2], Baylor College of Medicine, Houston, TX and Institut für Pharmakologie und Toxikologie[3], Braunschweig, Germany

ATP-sensitive K^+ channels, K_{ATP}, with the properties of the native pancreatic β-cell K_{ATP} channel, are generated by co-expression of SUR1, an ATP-binding cassette (ABC) superfamily member and $K_{IR}6.2$, an inwardly rectifying K^+ channel subunit. Both subunits are photolabeled by ^{125}I-azidoglibenclamide, a 4-azidosalicyloyl analog of glibenclamide, in membranes or after digitonin solubilization. Labeling of $K_{IR}6.2$ is dependent on co-expression with SUR1 indicating close association. $K_{IR}6.1$ also forms K_{ATP} channels with SUR1 and will co-photolabel. Both K_{IR} subunits, $K_{IR}6.x$, form digitonin stable complexes with SUR1 which can be purified by lectin chromatography, or using Ni^{2+}-agarose and a functional his-tagged SUR1. Co-expression with $K_{IR}6.x$ affects the glycosylation, generating core (140 K) and complex (150-170 K) glycosylated receptors, both species are found in α- and β-cell lines. Co-expression of SUR1 with $K_{IR}1.1$ (ROMK1) or $K_{IR}3.4$ (CIR) does not generate K_{ATP} channels and neither K_{IR} subunit photolabels, indicating there is a specificity of SUR1 interaction with the K_{IR} family. The estimated mass of the SUR1/$K_{IR}6.2$ complex, ~ 1000 kDa, is consistent with a tetrameric organization, $(SUR1/K_{IR}6.2)_4$, of K_{ATP} channels. The data define a new ion channel architecture consisting of an ABC superfamily protein interacting with specific inward rectifier K^+ channel subunits.

M-AM-G9

A STRUCTURAL MODEL FOR INTACT ANIONIC PHOSPHOLIPID REGULATION OF INWARDLY RECTIFYING K+ CHANNELS

((**Z. Fan**, B. Ye, J. C. Makielski)) University of Wisconsin, Madison, WI

The mechanism for run-down, a general characteristic of many members of the inwardly rectifying K+ channel family (Kir), is unclear. Several hypothesis, most involving protein phosphorylation, have been proposed, but none adequately explain available experimental evidence. We have recently shown that negatively charged phospholipids (NCPs) activate and maintain sustained activation of native ATP-sensitive K+ channels (K.ATP) from a variety of tissues, and also a K.ATP cloned from rat pancreas (co-expressed rSUR/rKir6.2) We propose a model in which highly conserved positive charges on the C-terminus of the channel protein interfaces with anionic head groups in the NCPs (or other anionic groups on or near the membrane) to keep Kir open. In support of this model, NCPs activated other members of Kir, including a human Kir1.1 and a mouse Kir2.1. When two charges at position 176 and 177 were neutralized (RR176AA) in Kir6.2, the effects of NCPs were reduced, and a mutant with a negative charge substituted (R176E) was inactive. Our results, and our model, suggest an important role for negatively charged membrane phospholipids in Kir activity, and maintenance of phosphorylated lipids may represent a novel regulatory mechanism for K.ATP and other Kir channels.

E-C COUPLING - DHPR AND RyR

M-AM-H1

LUMENAL Ca^{2+} CAN ACTIVATE THE SUB-OPTIMAL, CYTOSOLIC Ca^{2+}-ACTIVATED RABBIT SKELETAL MUSCLE Ca^{2+} RELEASE CHANNEL.

((Ashutosh Tripathy and Gerhard Meissner)) Departments of Biochemistry and Biophysics, and Physiology, University of North Carolina,Chapel Hill, NC 27599.

Previously, we have demonstrated that increasing lumenal Ca^{2+} from <μM to mM levels can activate and then inactivate the ATP-activated Ca^{2+} release channel (CRC) by having access to cytosolic Ca^{2+}-activation and inhibition sites (*Biophys. J.* 70:2600-2615, 1996). In this report, we provide experimental evidence that even in the absence of ATP, lumenal to cytosolic Ca^{2+} fluxes can activate the sub-optimal, cytosolic Ca^{2+}-activated CRC under appropriate conditions. Channel activities were recorded in 750 mM KCl solutions after incorporation of purified CRC in planar lipid bilayer membranes. A raise in [KCl] from 250 mM to 750 mM in recording solutions containing < μM to mM cytosolic Ca^{2+} increased the Hill inactivation constant (Ki) for Ca^{2+} from ~200 μM to ~5 mM with little change in the Hill activation constant (Ka, ~10 μM), thus widening the "Ca^{2+} window" of Ca^{2+} activation. Maintaining cytosolic Ca^{2+} at sub-optimal levels (0.5 - 1.5 μM) and increasing lumenal Ca^{2+} to mM levels resulted in substantial increase in channel activity at -40 mV (lumenal side, ground). Higher lumenal Ca^{2+} was needed to increase channel activity at +40 mV. Ca^{2+} fluxes up to ~2 pA increased channel activity. Inhibition of channel activity was observed with Ca^{2+} fluxes greater than ~8 pA. These data can be explained in terms of lumenal Ca^{2+} having access to cytosolic Ca^{2+} activation and inhibition sites. Supported by NIH.

M-AM-H2

BASTADIN 10 STABLIZES THE FULL CONDUCTANCE CONFORMATION OF THE SKELETAL SR Ca^{2+} RELEASE CHANNEL AND ELIMINATES ITS DEPENDENCE ON *CIS* Ca^{2+}

((**I.N. Pessah***, L. Chen*, T. Lam*, T.F. Molinski+, and E.D. Buck*)) *Department of Molecular Biosciences, School of Veterinary Medicine, and Department of Chemistry, University of California, Davis, CA 95616

Bastadin 10, a macrocyclic bromotyrosine derivative from *Ianthella basta,* was found to posses unprecedented activity toward the Ca^{2+} release channel (Ry_1 receptor) from skeletal muscle. Ca^{2+} fluxes from actively loaded junctional SR vesicles were measured using the metallochromic dye antipyrylazo III. Bastadin 10 releases accumulated Ca^{2+} even when the extravesicular free Ca^{2+} is <100nM without inhibiting the SERCA pump (ED_{50} = 5μM). Bastadin 10-induced efflux is inhibited by known Ry_1 channel blockers (μM ryanodine and ruthenium red). Importantly, the actions of bastadin 10 are fully negated by treatment of the vesicles with FK506 (50μM) even though the channel remains responsive to caffeine. The actions of bastadin 10 on single channel kinetic behavior were examined in bilayer lipid membranes with 5:1 (*cis:trans*) Cs^+ as the current carrier.

Free Ca^{2+} *cis* (μM)	Bastadin 10 (μM)	open probability (Po)
7.0	0	0.22
7.0	1. 5	0.54
7.0	3.0	0.77
7.0	4.5	0.91
7.0	7.5	0.92
0.083	7.5	0.96

Bastadin 10 (7.5μM) added to the *cis* chamber containing 7 μM Ca^{2+} immediately stabilized the full open conductance state of the channel raising Po to 0.92. The bastadin modified channel maintained its high Po, failing to exhibit adaptation for the duration of experiments typically lasting 5-20 min. EGTA added to the *cis* side revealed the channel was no longer under Ca^{2+} regulation in the physiological Ca^{2+} range. These results demonstrate that bastadin 10, through its modulatory action on the FKBP12/Ry_1 receptor complex can relieve the Ca^{2+} requirement for channel activation and eliminate channel adaptation.

M-AM-H3

FUNCTIONAL NON-EQUALITY OF THE CARDIAC AND SKELETAL RYANODINE RECEPTORS.

((**J.Nakai** [1,2], T. Ogura[2], F. Protasi[3], C. Franzini-Armstrong[3], P.D. Allen[4,5] & K.G. Beam[2])) [1]Natn. Inst. for Physiol. Sci., Japan; [2]Colorado St. Univ.; [3]Univ. of Pennsylvania; [4]Children's Hospital, Boston; [5]Brigham & Women's Hospital, Boston.

In previous work, we demonstrated that dyspedic skeletal muscle cells, which do not express the skeletal isoform of the ryanodine receptor (RyR-1), lack excitation-contraction (E-C) coupling, and have an ~30-fold reduction in L-type Ca^{2+} current density; both are restored by injection of RyR-1 cDNA. Thus, there appears to be reciprocal signalling between the skeletal dihydropyridine receptor (DHPR) and RyR-1 such that Ca^{2+} release activity of RyR-1 is controlled by the DHPR and the Ca^{2+} channel activity of the DHPR is controlled by RyR-1. Here we have examined the ability of the cardiac RyR (RyR-2) to substitute for RyR-1 in this interaction with the skeletal DHPR. When RyR-2 is expressed in dyspedic muscle cells, it gives rise to spontaneous intracellular Ca^{2+} oscillations and supports Ca^{2+}-entry-induced Ca^{2+} release. Electronmicrographs reveal that RyR-2 is expressed at junctions between sarcolemma and sarcoplasmic reticulum. However, unlike RyR-1, the expressed RyR-2 does not increase the Ca^{2+} channel activity of the DHPR, nor is the gating of RyR-2 controlled by the skeletal DHPR. Thus, the ability to participate in skeletal-type reciprocal signalling appears to be a unique feature of RyR-1. (Supported by Ministry of Education, Science, Culture & Sports, Japan and NIH)

M-AM-H4

EXPRESSION AND KNOCKOUT OF THE RYANODINE RECEPTOR TYPE 3 (RYR3) CALCIUM RELEASE CHANNEL GENE.

((D. Rossi[1], F. Bertocchini[1], A. Conti[1], V. Barone[1], **V. Sorrentino**[1,2])) [1]DIBIT, Istituto Scientifico HSR, Milano and [2]University of Siena, Italy.

Skeletal muscle fibers, neurons and other cells express more than one of the three known ryanodine receptors/calcium release channel genes. Several sites which undergo a process of alternative splicing have been identified in the three ryanodine transcripts. This process provides a further level of heterogeneity through which from each member of this family of calcium relase gene various functionally distinct channels may be generated in a given cell. We have recently produced mice lacking the expression of a functional ryanodine receptor type 3 isoform (RyR3). Analysis of these mice with respect to sites of expression such as the central nervous system and skeletal muscle cells, among others, is expected to provide some hints on the importance of expressing more than one isoform of RyR calcium channel in mammalian cells.

M-AM-H5

EXPRESSION AND FUNCTIONAL ANALYSIS OF RY_1R cDNA IN A MYOGENIC CELL LINE LACKING NATIVE RY_1R PROTEIN EXPRESSION

((**R.A. Moore***, I.N. Pessah*, and P.D. Allen#*)) *Dept. of Molecular Biosciences, School of Veterinary Medicine, University of California, Davis, CA 95616, #*Department of Anesthesia, Brigham and Women's Hospital, Boston, MA, and *Department of Cardiology, Children's Hospital, Boston, MA 02147

Ry_1 receptor (-/-) "knockout" 1B5 cell line exhibits uniform expression of myoD, myosin heavy chain, and desmin antigens upon differentiation in 5% heat-inactivated horse serum for 5-10 days. Differentiated fused 1B5 myotubes have been shown to express key triadic proteins by Western blot analysis, including triadin, calsequestrin, FKBP-12, SERCA1 and DHPR but do not express Ry_1, Ry_2, and Ry_3 receptor. Ratio flourescence imaging measurements of intracellular Ca^{2+} with fura-2, AM loaded cells reveal that differentiated 1B5 myotubes exhibit no response to caffeine (10-100 mM), 4-Chloro-m-cresol (500 μM -1 mM), thapsigargin (1μM) or ryanodine (50-500 μM). Control, similarly derived, 1D5 (Ry_1 receptor +/+) myotubes, do respond predictably to caffeine (10-100 mM), 4-Chloro-m-cresol (500 μM -1 mM), and ryanodine (50-500 μM). Transient transfection of 1B5 cells with pCMVRyR restores the presence of Ry_1 protein as demonstrated using in situ immunohistochemistry. Furthermore Ry_1 receptor function can be efficiently restored within 3-5 days post-transfection, as demonstarted by responsiveness to 4-Chloro-m-cresol (500 μM -1 mM) and ryanodine (50-500 μM). The 1B5 cell line provides a valuable model in which to study Ry_1 receptor structure and function in a homologous expression system.

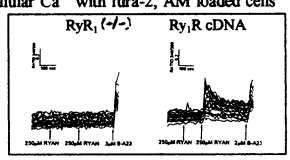

M-AM-H6

DIHYDROPYRIDINE RECEPTORS ARE CLUSTERED BUT DO NOT FORM TETRADS IN PERIPHERAL COUPLINGS OF DYSPEDIC MYOTUBES.

((**Feliciano Protasi***, Clara Franzini-Armstrong* and Paul D. Allen^)) *Dept. of Cell Dev. Biol., U. PA., Philadelphia, PA; ^Dept. of Anesth. Brigham and Women's Hospital, Boston, MA.

E-c coupling requires interactions between sarcoplasmic reticulum (SR) and the exterior membranes. Two proteins, essential to e-c coupling, face each other at SR-surface junctions: the ryanodine receptor (RyR1), or SR calcium release channel, and the dihydropyridine receptor (DHPR), or L type calcium channel. RyRs form arrays of feet, and, in skeletal muscle, they are associated with tetrads constituted of four DHPRs. A null mutation of RyR1 (the skeletal type) results in dyspedic skeletal muscle fibers, that lack e-c coupling (Takeshima et al., 1994, Nature, 369: 556, Nakai et al. 1996 Nature 380: 72-75), feet and tetrads (Takekura et al., 1995, Proc. Natl. Acad. Sci., 92: 3381). We obtained a dyspedic myoblast cell line (1B5) by MyoD conversion of fibroblasts from teratocarcinomas produced by homozygous ES cells which were similarly targeted. Using a combination of immuno-histochemistry and thin sectioning we find that, in differentiated cells, α_1 and α_2 subunits of the DHPR and triadin are clustered in small surface membrane patches and that the cells have "dyspedic" (no feet) peripheral couplings. In freeze-fracture (FF) replicas, numerous clusters of large intramembrane particles are seen. The particles are identified as DHPRs, based on similar location of DHPR foci detected by antibodies and clusters of particles seen by FF. DHPRs of dyspedic myotubes are not grouped into tetrads, differently from normal skeletal muscle, but similarly to cardiac muscle. Thus the absence of RyR1 does not impede the clustering of DHPRs at junctional sites, indicating that other proteins must be involved in holding DHPRs in the region facing the SR. This may also be the case in cardiac muscle, where DHPRs are clustered at the junctions but in positions not directly related to the feet. On the other hand, the formation of tetrads does require anchoring of DHPRs to feet, thus supporting the hypothesis of a direct interaction between the two molecules during e-c coupling. The presence of triadin in dyspedic junctions does not solve the question of whether or not this protein is needed for anchoring DHPRs to RyRs. We thank Dr. A. H. Caswell for the α–triadin antibody.

M-AM-H7

FUNCTIONAL EXPRESSION OF cDNA ENCODING THE TYPE 3 RYANODINE RECEPTOR OF RABBIT UTERUS IN HEK293 CELLS.

((**S. R. Wayne Chen**, Xiaoli Li and Lin Zhang)) Dept. of Med. Biochem., University of Calgary, Calgary, Alberta, Canada, T2N 4N1

Using reverse transcription polymerase chain reaction, DNA sequence analysis and RNase protection assay, we have identified several putative alternatively spliced variants of the type 3 ryanodine receptor (RyR3) in rabbit uterus. To study the functions of these putative alternatively spliced variants of RyR3, we have constructed full length cDNAs encoding each of these variants. One of these full length cDNAs containing a deletion of 15 bp (10021-10035) was transiently expressed in HEK293 cells. Western blotting and sedimentation analysis showed that this recombinant RyR3 variant migrated as a high molecular weight band in SDS-PAGE and formed a large oligomeric complex in a sucrose density gradient. Single channel properties of the recombinant RyR3 variant was investigated by using single channel recordings in planar lipid bilayers. The recombinant channel was activated by micromolar Ca^{2+}, millimolar ATP and caffeine, inhibited by Mg^{2+}, and modified by ryanodine. The recombinant RyR3 channel exhibited a conductance similar to that of RyR1, but the kinetics and response to millimolar Ca^{2+} were different from those of RyR1. The expression and single channel properties of other putative RyR3 variants are currently under investigation. (Supported by the MRC of Canada and AHFMR)

M-AM-H8

TARGETING OF THE DHP-RECEPTOR β SUBUNIT TO THE TRIAD DEPENDS ON INTERACTIONS WITH THE α_1 SUBUNIT.

((B. Neuhuber, F. Döring, H. Glossmann, T. Tanabe, and **B.E. Flucher**)) Institute of Biochemical Pharmacology, Univ. Innsbruck, Austria, and Dept. Cellular & Molecular Physiology, Yale Univ. School of Medicine, New Haven, CT.

Myotubes from the homozygous dysgenic cell line GLT can form junctions between T tubules (TT) and sarcoplasmic reticulum (SR) with normally incorporated ryanodine receptors despite the lack of the dihydropyridine receptor (DHPR) α_1 subunit. The skeletal muscle α_1 subunit was expressed from a plasmid ($pC\alpha_{1S}$) in GLT myotubes with and without a fusionprotein of the DHPR β subunit and the green fluorescent protein (βGFP) and was subsequently localized by immunofluorescence labeling. The α_1 subunit became incorporated into the TT/SR junctions as seen by its clustered distribution pattern and its colocalization with the ryanodine receptor. In the absence of α_1 the β subunit failed to get incorporated into the junctions. βGFP was diffusely distributed throughout the cytoplasm and showed no association with any identifiable membrane system. However, upon co-expression with the α_1 subunit, βGFP displayed a clustered distribution pattern. The βGFP clusters colocalized with immunolabel of the α_1 subunit and the ryanodine receptor, indicating a junctional location. Co-expression of βGFP and a α_1 subunit in which the β-interaction domain has been deleted ($pC\alpha_{1S}$-$\Delta_{351\text{-}380}$) did neither lead to a junctional location of βGFP nor of the mutated α_1 subunit. Thus, in skeletal muscle association of the α_1 and β subunits of the DHPR via the β-interaction domain in the I-II cytoplasmic loop of α_1 is required for the incorporation of the Ca^{2+} channel complex into the triad junction.

(Supported by FWF grants S06601, S06612, and an APART Fellowship from the Austrian Acad. Sci.)

MEMBRANE FUSION: EXOCYTOSIS AND ENDOCYTOSIS I

M-AM-I1

DEVELOPMENT OF pH-SENSITIVE LIPOSOMES COMPOSED OF A NOVEL "CAGED" DIOLEOYLPHOSPHATIDYLETHANOLAMINE.

((**D. C. Drummond** and D. L. Daleke)) Dept. of Chemistry and Dept. of Biochem. and Mol. Biology, Indiana Univ., Bloomington, IN 47405 USA.

We have used reversibly *N*-modified derivatives of dioleoylphosphatidylethanolamine (DOPE) to construct pH-sensitive liposomes. The citraconyl blocking group used in these studies was previously shown to be pH-labile (Drummond & Daleke, *Chem. Phys. Lipids* 75 (1995) 27-41). This property provides a unique mechanism for "caging" an important biophysical characteristic of DOPE: its ability to form fusion-competent nonbilayer structures. In the present work, we evaluate the potential of this lipid as a tool to study membrane fusion and develop pH-sensitive drug delivery vehicles. Using ^{31}P NMR spectroscopy, citraconyl-DOPE (cit-DOPE) was found to stabilize DOPE in the bilayer form at concentrations of 10 mol% or greater. However, extended incubations (60 min, 37 °C) at low pH (5.0) resulted in the appearance of hex II phase and other more isotropic nonbilayer structures. The fusogenic properties of DOPE:cit-DOPE (9:1) large unilamellar vesicles (formed by freeze-thaw and extrusion through 100 nm filters) was studied using fluorescent contents (calcein) and lipid (N-Rh-PE/N-NBD-PE) markers. At neutral or slightly basic pH these liposomes stably encapsulated calcein. Leakage was shown to be dependent on temperature, pH, and calcium. The effects of calcium and pH were synergistic. Lipid mixing, as measured by fluorescence energy transfer between N-Rh-PE and N-NBD-PE, was also dependent on pH and calcium. However, when DOPC was substituted for DOPE, no lipid mixing occurred. Finally, DOPE:cit-DOPE liposomes were also shown to deliver calcein to the cytosol of cultured CV-1 cells. The results described here demonstrate a novel method for the preparation of pH-sensitive liposomes with the potential for the cytoplasmic delivery of drugs and oligonucleotides to target cells. These and other possibilities are presently being examined.

M-AM-I2

STRUCTURAL STUDY OF THE RELATIONSHIP BETWEEN THE INFECTIVITY OF INFLUENZA VIRUS AND THE ABILITY OF ITS FUSION PEPTIDE TO PERTURB BILAYERS.

((**A. Colotto and R.M. Epand**)) McMaster University, Dept. of Biochemistry, Hamilton, Ontario, L8N 3Z5, Canada.

The amino terminal segment of the HA2 protein of influenza virus (fusion peptide) has been identified as an important region for membrane fusion. The wild type virus can fuse to membranes more rapidly at pH 5 than at pH 7.4. It has been demonstrated that there is a relation between the ability of the peptide to promote the formation of inverted phases and the fusogenicity of the intact virus. In this work, we use small-angle X-ray diffraction to elucidate the structural nature of the perturbations caused by the fusion peptide on two lipid systems: (i) monomethyl-dioleoylphosphatidylethanolamine (MeDOPE); and (ii) dipalmitoleoylphosphatidylethanolamine (DPOPE). Measurements of the peptide effects were made at peptide to lipid molar ratios of 0.01 and 0.001. At pH 5 striking effects are observed for both lipids. There is rapid appearance of a cubic phase for MeDOPE. A cubic phase was also observed with DPOPE, which had not been previously observed with this lipid in pure form. At pH 7.4, the effects on MeDOPE are greater than on DPOPE. For MeDOPE, the L_α d-spacing increases by 8 Å compared to ca 2 Å for DPOPE. Also, the d-spacing of the H_{II} phase is greatly increased in the MeDOPE system. The present results support the idea that there is a relation between the ability of the peptide to promote the formation of inverted phases, particularly the cubic phase, and the fusogenicity of the intact virus.

M-AM-I3

WILD-TYPE HA INDUCES HEMIFUSION BETWEEN CELL MEMBRANES.

((V.A.Frolov[1,2], E.Leikina[1], P.Bronk[1], L.Chernomordik[1], J.Zimmerberg[1]))
[1] LTPB, NICHD, NIH, Bethesda, MD, 20892,
[2] A.N.Frumkin Institute of Electrochemistry, Russian Academy of Science, Moscow, Russia.

Hemagglutinin (HA), the fusogenic protein of the Influenza viral envelope, is both necessary and sufficient for fusion of virus to cells and between cells. A mutant of HA causes hemifusion of membranes, in which lipids mix but no fusion pores are formed. Here we report that wild type HA, under certain conditions, also has the ability to produce hemifusion. Using simultaneous video-enhanced fluorescence microscopy and time- resolved admittance measurements, we studied low-pH triggered fusion between lipid-dye labeled human erythrocytes (RBCs) and HAb2 fibroblasts expressing HA (HAb2 cells). wtHA induced hemifusion when the temperature of the medium was decreased (down to 20C) and when less acidic solutions triggered the conformational changes of HA molecules (pH 5.3). In 4/13 trials at 33C, pH 5.3 and in 3/14 trials at 20C, pH 4.9 substantial membrane dye exchange was detected despite a complete absence of fusion pore conductance, within our limit of detection of 50 pS for 5 ms. In these trials when fusion pores occurred, they never enlarged their conductance above 1.5 nS. In fluorometry experiments with RBCs labeled by both aqueous and lipid dyes, the efficiency of aqueous dye exchange for non-optimal temperatures and pH values was much lower than that of membrane dye exchange. Thus wtHA does not always induce complete fusion which culminates in full enlargement of the fusion pore, but also is able to cause hemifusion and partial pore opening.

M-AM-I4

FACILITATION Ca CHANNELS ARE RECRUITED BY ACTION POTENTIALS IN CALF ADRENAL CHROMAFFIN CELLS AND MEDIATE "STRONG COUPLING" BETWEEN Ca ENTRY AND CATECHOLAMINE SECRETION.

((A. Elhamdani[1], Z. Zhou[2] and C. R. Artalejo[1])). [1]Dept. Pharmacol., Wayne State Univ., MI, Detroit, MI 48201; [2]Dept. Physiol., Loyola Univ., IL 60153. (Spon by P. Loach).

ACh released from the splanchnic nerve elicits depolarization and trains of action potentials (APs) in adrenal chromaffin cells in situ. To simulate this physiological situation we used APs and trains of AP waveforms (APWs) to trigger secretion in cultured calf chromaffin cells. Secretion was quantitated by amperometric detection of released catecholamines and capacitance measurements. To characterize AP-induced quantal release of catecholamines we stimulated at frequencies of 1 and 7 Hz and analysed the resultant latency histograms. At 1 Hz, >90% of amperometric spikes occur with a delay of 1-20 msec ("strongly-coupled") but at 7 Hz, only ~50% of events occur with a latency of <20 msec while the other ~50% occur with latencies of 60-140 msec ("loosely-coupled"). The decay of the early peaks in the 1 and 7 Hz histograms has a time constant of about ~4.5 and ~7.6 msec respectively. Nisoldipine knock out the strongly-coupled signal while the polypeptide toxins eliminate the loosely-coupled signal. We hypothesize that strong-coupling reflects the proximity of facilitation L-type Ca channels and release sites, while loose-coupling reflects the activity of N- and P-type channels that are distant from the release sites. These findings corroborate our previous results and strongly suggest that the facilitation Ca channels may underly the massive catecholamine release that occurs during the "fight or flight" response (Artalejo, et al., Nature 367, 72, 1994). In addition, they serve to underscore the difference between calf and adult bovine chromaffin cells: the later do not have facilitation Ca channels and show only the loosely coupled mode of secretion (Chow et al, Neuron, 16, 369, 1996) (Supported by NIH).

M-AM-I5

EXOCYTOSIS OF AND CATECHOLAMINE RELEASE FROM SINGLE CHROMAFFIN GRANULES MEASURED BY PATCH AMPEROMETRY.

((A. Albillos[1,2], G. Dernick[1], G. Alvarez de Toledo[3] and M. Lindau[1])). [1]Dept. Molecular Cell Research, MPI f. Medical Research, D-69120 Heidelberg, Germany; [2]Dept. Pharmacology & Therapeutics, Autonomous Univ., E-28029 Madrid, Spain; [3]Dept. Physiology & Biophysics, Univ. of Seville, E-41009 Sevilla, Spain.

Exocytosis of single chromaffin granules was studied in bovine chromaffin cells using patch amperometry. Capacitance measurements and amperometric detection of catecholamine release with a carbon fiber electrode were performed simultaneously in the cell attached patch clamp configuration. In 10% of patches spontaneous capacitance steps associated with amperometric transients indicated exocytosis of chromaffin granules. Step sizes ranged from 0.7 fF to 14 fF. The charge estimated from the integrated amperometric transients ranged from 0.4 pC to 17 pC and was correlated with step size. The step size distribution showed peaks at 1.5 and 4.4 fF. The first peak agrees with morphometric data (Horstmann & Almers unpublished) but the number of large steps was larger than expected, suggesting that they reflect compound exocytosis. In vesicles with step size <2.5 fF the average catecholamine concentration was about 1 M. Exocytosis of chromaffin granules occurred spontaneously after patch formation. After steps had ceased, patch depolarization did not induce further capacitance steps. Similarly, in patches showing no spontaneous activity, depolarization did not stimulate any capacitance step or amperometric transient. Thus, in patches with exocytotic competence, sealing of the patch pipette stimulates exocytosis of all releasable granules. Several amperometric signals were preceded by a foot. We show that the foot is due to release through a narrow fusion pore with conductance <1 nS. Upon pore expansion the rate of release increases markedly. This result shows that the kinetics of catecholamine release following fusion pore formation is initially limited by the fusion pore and not by dissociation from the granular matrix.

M-AM-I6

INFORMATION TRANSFER AT A SYNAPSE - INSIGHTS FROM SIMULTANEOUS AMPEROMETRIC AND POSTSYNAPTIC MEASUREMENTS OF SINGLE VESICLE RELEASE.

((S. Sivaramakrishnan and J. M. Fernandez)). Physiology & Biophysics, Mayo Clinic, Rochester, MN 55905.

Complete and transient fusion of secretory granules with the plasma membrane of mast cells results in the release of serotonin from single vesicles. When a carbon fiber is used to measure serotonin release, complete fusion of a single vesicle results in an amperometric 'spike' which is sometimes preceded by a small, slow leak of transmitter, called a 'foot'. Transient fusion does not cause a spike, but results in a 'flicker' of serotonin release. To examine the relative importance of the spike, the flicker and the foot in the transfer of information from one cell to another, such as occurs at a synapse in the nervous system, we have combined amperometric detection of single vesicle release with whole-cell patch clamp recordings from 'postsynaptic' cells expressing serotonin receptors and held in close apposition to a mast cell, forming a pseudo-synapse. These postsynaptic cells (N1E115 and NG108-15) were derived from neuroblastoma-glioma cell lines and expressed the 5HT3 sub-type of serotonin receptor.

At the mast cell-N1E115 synapse, single vesicles did not cause postsynaptic responses. Instead, a burst of several single release events was necessary to trigger a postsynaptic current, which was prolonged and which occurred after a significant delay from the first vesicle released. The postsynaptic current decayed to baseline in the continued presence of vesicle release, suggesting desensitization of the postsynaptic receptors. To examine the postsynaptic response to single release events, we used the beige mouse mast cell-NG108-15 synapse. At this synapse, each amperometric spike, corresponding to the complete fusion of a single vesicle, was translated into a single excitatory postsynaptic current. In some cases, the postsynaptic cell also responded to the foot and the flicker, though the responses were small. When the time between single release events was short, postsynaptic currents occurred in response to the first two or three vesicles released, after which the postsynaptic cell was unresponsive for a while and then began to respond again to single release events. Using rapid perfusion techniques to better control the shape and concentration of serotonin at postsynaptic receptors, we are examining the role of desensitization and other factors which may shape the translation of a release event into a postsynaptic response.

M-AM-I7

PLASMA MEMBRANE DYNAMICS IN RAT PERITONEAL MAST CELLS STUDIED BY PATCH AMPEROMETRY.

((E. Alés, L. Tabares, M. Lindau* and G. Alvarez de Toledo)). Dept. Physiology and Biophysics. Univ. of Seville. E-41009, Sevilla. Spain, and *Dept. Molecular Cell Research, MPI f. Medical Research, D-69120 Heidelberg, Germany. (Spon. by S. Sala)

Plasma membrane dynamics due to exocytosis and endocytosis were studied in rat peritoneal mast cells using patch amperometry. Capacitance measurements were performed in the cell attached configuration of the patch clamp technique. Amperometric detection of serotonin release from the membrane patch was obtained simultaneously with a carbon fiber electrode introduced into the patch pipette. After seal formation two types of events were obtained spontaneously and clearly distinguished. Small step increases in capacitance (0.17 ± 0.11 fF, mean ± s.d.) and relatively large capacitance events (15-60 fF). Small membrane fusion events were not accompanied by a detectable amperometric transient, probably indicating the fusion of small clear core vesicles. Some of these events were intermixed with back steps of the same amplitude that could correspond to endocytosis. The large events showed a typical amperometric spike due to the release of serotonin, indicating the fusion of mast cell granules with the plasma membrane. Because of the relatively large granule capacitance of some of these events and the 8 KHz frequency used in our records, the fusion pore conductance could be calculated while developing the amperometric transient. The correlation between fusion pore conductance and amperometric current was linear during the upstroke of the spike, indicating that during this phase the pore is limiting for release. After the spike has reached its maximum amplitude the pore continues to grow. At that stage the kinetics for release seems to be governed by the binding properties of serotonin to the granule matrix.

M-AM-J1

PROTEIN AND LIPID STRUCTURAL CHARACTERISTICS ASSOCIATED WITH DISRUPTION OF THE PURPLE MEMBRANE CRYSTALLINE ARRAY: AN INFRARED SPECTROSCOPIC STUDY

((**Steven M. Barnett** and Ira W.Levin))
Laboratory of Chemical Physics, NIDDK, NIH, Bethesda, Maryland, 20892-0510.

Infrared spectroscopy was used to monitor protein and lipid reorganizations in purple membrane assemblies perturbed by exposure to Triton, by heating, by the release of retinal, and by the application of pressure. The conformational flexibility of bacteriorhodopsin, an integral membrane protein, is reflected by the temperature dependence of the frequencies and intensities of the protein amide I modes (~1660 cm^{-1}) while frequency shifts in the 1545 cm^{-1} protein amide II and 3303 cm^{-1} amide A modes are consistent with changes in water structure within the retinal binding cavity. The latter data emphasize the effects of the surrounding water on the changes in various bond force constants and in the coupling characteristics between vibrational modes within bacteriorhodopsin as the protein undergoes conformational changes during the photocycle. The intensity decreases in the protein amide II spectral interval and in the Fermi resonance 2927 cm^{-1} carbon-hydrogen stretching mode region which arise upon bilayer loss of retinal are indicative of reduced membrane lipid-lipid and lipid-protein interactions. Comparisons of native systems to purple membranes exposed either to light or to heat illustrate the molecular rearrangements that arise as the bilayer minimizes the membrane void volumes created by the loss of retinal. Since the purple membrane lipids serve to maintain the appropriate retinal-apoprotein spatial coupling between these two moieties and to support the well-ordered purple membrane crystalline array, a disruption of this coupling leads, in part, to the observed photocycle changes observed on exposure to Triton.

M-AM-J2

THE TERTIARY STRUCTURAL CHANGES IN BACTERIORHODOPSIN OCCUR BETWEEN M STATES: X-RAY DIFFRACTION AND FOURIER TRANSFORM INFRARED SPECTROSCOPY

((H.-J. Sass, I.W. Schachowa, G. Rapp, M.H.J. Koch, D. Oesterhelt, N.A. Dencher, & **G. Büldt**)) Forschungszentrum Jülich, IBI-2, 52425 Jülich, EMBL/DESY, 22603 Hamburg, MPI für Biochemie, 82152 Martinsried, Institut für Biochemie, TH Darmstadt, 64287 Darmstadt, FRG

The tertiary structural changes occuring during the photocycle of bacteriorhodopsin (BR) are assigned by X-ray diffraction to distinct M states M_1 and M_2. These light-dependent conformational changes of BR-Asp96Asn are observed at high hydration levels but not in partially dehydrated samples. The FTIR spectra of continuously illuminated samples at low and high hydration, despite some differences, are characteristic of the M intermediate. The changes in diffraction patterns of samples in the M_2 state are of the same magnitude as those of wild-type samples trapped in the M_G state with GuaHCl. Additional large changes in the amide bands of the FTIR spectra occur between M_2 and M_G. We suggest, that the tertiary structural changes between M_1 and M_2 are reponsible for the switch opening the cytoplasmic half channel of BR for reprotonation to complete the catalytic cycle. These tertiary structural changes seem to be triggered by a charge redistribution which might be a common feature of retinal proteins also in signal transduction.

M-AM-J3

ELECTRIC-FIELD-INDUCED SCHIFF-BASE DEPROTONATION IN DRY FILMS OF D85N MUTANT BACTERIORHODOPSIN.

((**Paul Kolodner**[1], Evgeniy P. Lukashev[2], Yuan-chin Ching[1], and Denis L. Rousseau[3])) [1]Bell Laboratories, Lucent Technologies, Inc.; [2]Department of Biophysics, Moscow State University; [3]Department of Physiology and Biophysics, Albert Einstein College of Medicine (Sponsored by Winfried Denk)

We report measurements of the changes in the optical absorption spectra of dry films of wild-type and D85N mutant bacteriorhodopsin (BR) caused by the application of an external electric field. Oriented and unoriented films were used to examine the vectoriality of the electric-field effects. In wild-type BR, electric fields produce a red-shifted bathoproduct unrelated to changes in the protonation state of the Schiff base. In D85N mutant BR, electric fields cause deprotonation of the Schiff base in a fraction of the molecules, resulting in a partial shift of the optical absorption maximum from 600 nm to 400 nm. In both cases, the electric field induces a spectral change only in molecules with the correct orientation with respect to the applied field. The difference in the field effects seen in the wild-type and mutant proteins is correlated with the lower pK of the Schiff base in the mutant (pK ~ 9) compared with that in the wild type (pK ~ 13). Similar effects have been observed in other bacteriorhodopsin mutants and analogs with low Schiff-base pK's.

M-AM-J4

AZIDE AND OTHER WEAK ACIDS ACCELERATE THE DECAY OF THE LONG-LIVED O INTERMEDIATE IN THE BACTERIORHODOPSIN MUTANT GLU204GLN.

((R. Govindjee[1], **S. Misra**[1], T. G. Ebrey[1], N. Chen[2], J.-X. Ma[2], and R. K. Crouch[2])) [1]Center for Biophysics and Computational Biology, Univ. of Illinois at Urbana-Champaign, Urbana, IL 61801 and [2]Medical Univ. of S. Carolina, Charleston, SC 29425.

The second half of the photocycle of the bacteriorhodopsin mutant Glu204Gln is greatly slowed down compared to the wild type. Specifically, the decay of the O intermediate is slowed down approximately 10-fold relative to wild type O decay. Proton release to the extracellular solvent occurs during the O decay in this mutant, possibly directly from Asp85. We investigated whether the slow decay of O in this mutant is due to a slow rate of Asp85 deprotonation. We have found that millimolar concentrations of azide, formate and cyanate reduce the photocycling time of Glu204Gln to times typical of the wild type by accelerating the decay of O. The decay of O, monitored at 680 nm, and the coincident proton release, measured using the pH-sensitive dye pyranine, are accelerated to the same extent by azide. While the effect of azide did not vary with pH, the pH dependences of the effects of formate and cyanate suggest that the deprotonated forms of these acids are the active species in the acceleration of O decay. The temperature dependence of the weak acid effects suggests that weak acids decrease the activation barrier for Asp85 deprotonation by increasing the activation entropy rather than by lowering the activation enthalpy. It has previously been shown that azide and other weak acids can affect proton transfers in the cytoplasmic half of bacteriorhodopsin; here we show that they can act in the extracellular half of the protein as well.

M-AM-J5

VOLTAGE DEPENDENCE OF PROTON PUMPING IN BACTERIORHODOPSIN.

((G. Nagel, B. Kelety, G. Büldt*, & E. **Bamberg**))
Max-Planck-Institut für Biophysik, D-60596 Frankfurt
& *IBI-2, Forschungszentrum D-52425 Jülich, F.R.G.

Recently we reported successful expression of bR in *Xenopus* oocytes. The whole cell current of oocytes was measured 3 to 5 days after mRNA injection with a conventional two electrode voltage clamp setup. Whereas control oocytes (which were not injected), showed no current response upon illumunation with intense light (>550nm), mRNA injected oocytes developed a fast outward current response upon illumination. Light induced currents up to 100 nA were recorded at different test potentials, showing a strong voltage dependence in the investigated range of -165mV to +60mV. The light induced current does not invert at any of these voltages, as expected for a highly oriented membrane insertion. The quenching effect by blue light increases with increasing negative membrane potentials. At negative potentials two processes with different time constants for the M decay are observed (with 20 and 600 ms at neutral pH). Both decay times are virtually voltage independent, whereas the ratio of their corresponding amplitudes is strongly voltage dependent. The results are supported by determination of photocurrents induced by bR on planar lipid films where the pH dependence of the slow time constant confirms reprotonation of the Schiff base via the extracellular channel. This is strong evidence that the electrical field regulates the ratio between the M1 and the M2 intermediate thereby modulating the pump current.

(Supported by MPG and DFG.)

M-AM-J6

PHOTOINDUCED TRANSFORMATION OF 4-KETO-BACTERIORHODOPSIN GELATIN FILMS BASED ON BOTH WILD TYPE AND D96N MUTANT

(**A. B.Druzhko** and H.H. Weetall) BD, NIST, Gaithersburg, MD 20899.

Spectral and kinetic transformation studies of gelatin films based on 4-keto wild-type bacteriorhodopsin (BR) and 4-keto D96N mutant BR were carried out using absorbance spectroscopy. Spectral heterogeneity in 400 nm range, assumed to be associated with the M-intermediate state, previously characterized for films of 4-keto wild-type BR, was observed in the 4-keto D96N mutant BR. This heterogeneity is associated to a greater extent with chromophore replacement than with amino acid replacement. The time constants of the M-decay are larger for all kinetic components for 4-keto D96N mutant in the absence of sodium azide. In addition, the more long-lived component of the decay is almost twice as large for the film without sodium azide as it is for a film with sodium azide. This sodium azide effect on the kinetics is opposite to that observed in the 4-keto wild type BR. The comparison of the kinetics and spectral transformations of both pigments suggests that films containing 4-keto D96N mutant hold greater promise as media for information storage and retrieval.

M-AM-J7

PHOTORECEPTOR-TRANSDUCER MOLECULAR COMPLEX OF SENSORY-RHODOPSIN-I: A ROTATIONAL DIFFUSION STUDY.

((**R. A. Bogomolni**, J.G Fukushima, T. Swartz and I. Szundi)) Department of Chemistry and Biochemistry, University of California, Santa Cruz.

We used photoselection spectroscopy to probe the rotational motions of native sensory rhodopsin-I (sR-I) and of sR-I free of its transducer HtrI (tsR-I). We measured transient polarization anisotropy changes during the photocycles of sR-I and tsR-I in cell membrane pellets of wild-type and HtrI-deficient Halobacterium salinarum strains respectively, in which sR-I is the only photochemically-active pigment. As reported earlier (Biophys. J. 57 :539 (1990)) sR-I shows a flash-induced anisotropy decaying with half-times in the 30-300 microsecond range from initial values around 0.34 (theoretical maximum = 0.4) to non-zero limiting values around 0.1. In contrast tsR-I shows a rapidly decaying anisotropy ($t_{1/2}$< 30 microsec.) to a non-zero limiting value around 0.04-0.06. Analysis of the data in terms of restricted molecular motions around an axis perpendicular to the membrane plane are consistent with a model in which the rapidly-rotating tsR-I is perhaps a monomer or a small oligomer (the uncertainty originates mainly from our lack of knowledge of the local membrane viscosity). From the limiting anisotropy we calculate that the angle of its retinal chromophore with respect to the membrane plane is around 20°. Native sR-I, in contrast, shows significantly hindered motion as expected if it is bound to its transducer, as well as a different chromophore angle. Assuming similar membrane viscosity in the two strains, the long anisotropy decay times for native sR-I **cannot** be accounted for by a model in which sR-I and HtrI exist in a 1:1 ratio in the complex. Higer stoichimetries and/or interaction with other membrane or cytoplasmic proteins may be invoked.

M-AM-J8

RELAXATION DYNAMICS OF THE TWISTED CHROMOPHORE OF THE PRIMARY PHOTOPRODUCTS OF BACTERIORHODOPSIN AND HALORHODOPSIN.

((A. K. Dioumaev and **M. S. Braiman**)) Biochemistry Department, University of Virginia Health Sciences Center, Charlottesville, VA 22908.

We have analyzed the red-shifted photoproducts of bacteriorhodopsin (bR) and halorhodopsin (hR) on the ns time scale using step-scan Fourier transform infrared spectroscopy. Both the primary K photoproduct of bR and the corresponding hK photoproduct of hR are known to have significant twists in their retinylidene protonated Schiff base chromophores. We have characterized previously-unobserved relaxations in these twisted chromophore conformations occurring with time constants of $\tau_K \simeq$50–100 ns for K and $\tau_{hK} \simeq$250 ns for hK (measured at 20°C). These transitions are clearly distinguishable in the time-resolved IR spectral measurements from much-slower transitions to the L and hL photoproducts. We designate the earlier and later forms of the bR bathophotoproducts as K_E and K_L, and the corresponding hR photoproducts as hK_E and hK_L. The transitions between these 2 forms of K, and between the corresponding 2 forms of hK, have never been observed in visible spectroscopic measurements on the sub-μs time scale. Nevertheless, both the $K_E \rightarrow K_L$ and $hK_E \rightarrow hK_L$ transitions are characterized by substantial intensity decreases and frequency shifts of several vibrations of the chromophore's Schiff base, including the C=N stretch and the C_{15}-H out-of-plane wag.

Supported by NIH grant GM46854 and Fogarty Fellowship TW05212.

M-AM-J9

CRYSTALLOGRAPHIC STUDIES OF THE FIRST INTERMEDIATE IN THE PHOTOCYCLE OF THE BIOLOGICAL LIGHT SENSOR PHOTOACTIVE YELLOW PROTEIN (PYP).

Ulrich K. Genick, Ilona Canestrelli, Elizabeth D. Getzoff, Department of Molecular Biology, The Scripps Research Institute, La Jolla, California 92037, USA

The cis-trans isomerizations during the formation of the first intermediate in light cycles of many biological photoreceptors are among the fastest reactions in biology. Yet they take place in the densely packed interior of proteins. How is it possible to perform such fast reactions in a spatially restrained environment and still generate a chromophore geometry that is able to trigger the large scale structural rearrangements that occur in the later stages of protein photocycles? To answer these questions we use low temperature trapping combined with cryo-crystallography and ultrafast time-resolved Laue crystallography to determine the structure of the first intermediate in the light cycle of Photoactive Yellow Protein. PYP is a cytosolic photoreceptor from Ectothiorhodospira halophila that has proven unusually amenable to structural studies. We have previously determined the structure of PYP's ground state (Borgstahl et al.1995 *Biochemistry* 34, 6278-6287) and of the late intermediate (Genick et al. *Science* accepted). Difference electron density maps generated from our cryo-crystallographic experiments indicate that the changes during the formation of the early intermediate are restricted to the chromophore and indicate only minimal movement in PYP's *p*-hydroxycinnamyl chromophore.

SOCIETY AWARD WINNERS SYMPOSIUM

Awards-Sym-1 *1997 Young Investigator Award Winner*
D. W. Hilgemann, University of Texas SW Medical Center
Regulation of Ion Channels and Transporters by Inositol-Containing Phospholipids

Awards-Sym-2 *1996 Margaret Oakley Dayhoff Award Winner*
S. Marqusee, University of California, Berkeley
Dissection of the Protein Folding Problem: Studies of Partially Folded Proteins

Awards-Sym-3 *1997 Winner of the Avanti Award in Lipids*
C-h. Huang, University of Virginia
A Combined Calorimetric/Molecular Mechanics Investigation of Bilayers Composed of Saturated and/or Unsaturated Mixed-chain PC or PE

Awards-Sym-4 *1997 Elisabeth Roberts Cole Award Winner*
W. H. Woodruff, Los Alamos National Laboratory
Time-Resolved Vibrational Studies of the Fast Events in Protein Folding

Awards-Sym-5 *1997 Distinguished Service Award Winner*
T. D. Pollard, Salk Institute
Scientists as Political Advocates